43540

National Library of Canada | Bibliothèque nationale du Canada

Canadian Theses Division | Division des thèses canadiennes

Ottawa, Canada
K1A 0N4

PERMISSION TO MICROFILM — AUTORISATION DE MICROFILMER

• Please print or type — Écrire en lettres moulées ou dactylographier

Full Name of Author — Nom complet de l'auteur

FREDERICK C SALEVSKY

Date of Birth — Date de naissance

24/11/54

Country of Birth — Lieu de naissance

CANADA

Permanent Address — Résidence fixe

#01A/B 8901-112 St
EDMONTON, AB
T6G 2C5

Title of Thesis — Titre de la thèse

VORTICES IN THE GROUND STATE OF THE TWO-DIMENSIONAL SPIN $\frac{1}{2}$ XY MODEL

University — Université

UNIV. OF ALBERTA

Degree for which thesis was presented — Grade pour lequel cette thèse fut présentée

M.Sc.

Year this degree conferred — Année d'obtention de ce grade

1979

Name of Supervisor — Nom du directeur de thèse

DONALD D. BETTS

Permission is hereby granted to the NATIONAL LIBRARY OF CANADA to microfilm this thesis and to lend or sell copies of the film.

The author reserves other publication rights, and neither the thesis nor extensive extracts from it may be printed or otherwise reproduced without the author's written permission.

L'autorisation est, par la présente, accordée à la BIBLIOTHÈQUE NATIONALE DU CANADA de microfilmer cette thèse et de prêter ou de vendre des exemplaires du film.

L'auteur se réserve les autres droits de publication; ni la thèse ni de longs extraits de celle-ci ne doivent être imprimés ou autrement reproduits sans l'autorisation écrite de l'auteur.

Date

Oct 2/79

Signature

Fred C. Salevsky

NL-91 (4/77)

National Library of Canada

Cataloguing Branch
Canadian Theses Division

Ottawa, Canada
K1A 0N4

Bibliothèque nationale du Canada

Direction du catalogage
Division des thèses canadiennes

NOTICE

The quality of this microfiche is heavily dependent upon the quality of the original thesis submitted for microfilming. Every effort has been made to ensure the highest quality of reproduction possible.

If pages are missing, contact the university which granted the degree.

Some pages may have indistinct print especially if the original pages were typed with a poor typewriter ribbon or if the university sent us a poor photocopy.

Previously copyrighted materials (journal articles, published tests, etc.) are not filmed.

Reproduction in full or in part of this film is governed by the Canadian Copyright Act, R.S.C. 1970, c. C-30. Please read the authorization forms which accompany this thesis.

THIS DISSERTATION
HAS BEEN MICROFILMED
EXACTLY AS RECEIVED

AVIS

La qualité de cette microfiche dépend grandement de la qualité de la thèse soumise au microfilmage. Nous avons tout fait pour assurer une qualité supérieure de reproduction.

S'il manque des pages, veuillez communiquer avec l'université qui a conféré le grade.

La qualité d'impression de certaines pages peut laisser à désirer, surtout si les pages originales ont été dactylographiées à l'aide d'un ruban usé ou si l'université nous a fait parvenir une photocopie de mauvaise qualité.

Les documents qui font déjà l'objet d'un droit d'auteur (articles de revue, examens publiés, etc.) ne sont pas microfilmés.

La reproduction, même partielle, de ce microfilm est soumise à la Loi canadienne sur le droit d'auteur, SRC 1970, c. C-30. Veuillez prendre connaissance des formules d'autorisation qui accompagnent cette thèse.

LA THÈSE A ÉTÉ
MICROFILMÉE TELLE QUE
NOUS L'AVONS REÇUE

THE UNIVERSITY OF ALBERTA

VORTICES IN THE GROUND STATE OF THE TWO-DIMENSIONAL SPIN ½ XY MODEL

by

© FRED C. SALEVSKY

A THESIS

SUBMITTED TO THE FACULTY OF GRADUATE STUDIES AND RESEARCH

IN PARTIAL FULFILMENT OF THE REQUIREMENTS FOR THE DEGREE

OF MASTER OF SCIENCE

IN

THEORETICAL PHYSICS

DEPARTMENT OF PHYSICS

EDMONTON, ALBERTA

FALL, 1979

THE UNIVERSITY OF ALBERTA

FACULTY OF GRADUATE STUDIES AND RESEARCH

The undersigned certify that they have read, and recommend to the Faculty of Graduate Studies and Research, for acceptance, a thesis entitled VORTICES IN THE GROUND STATE OF THE TWO-DIMENSIONAL SPIN ½ XY MODEL submitted by FRED C. SALEVSKY in partial fulfilment of the requirements for the degree of Master of Science in Theoretical Physics.

Donald R. Betts

Supervisor

Bruce L Clarke

Date Sept. 7/79

It is not at all true that the scientist goes after the truth. It goes after him.

Sören Kierkegaard

ABSTRACT

The study of phase transitions in two-dimensional systems which possess more than one degree of freedom has been propelled by apparently contradictory evidence for the existence of such transitions. The situation was clarified by the work of Kosterlitz and Thouless who introduced the idea of topological long-range order to replace the more familiar concept. The phase transition in, for example, the classical ($s=\infty$) XY or plane rotator model is then viewed as corresponding to the unbinding of pairs of topological excitations (vortices and antivortices). Such a picture has inspired much theoretical work and has been experimentally confirmed. This thesis is the beginning of a study of the nature of the phase transition in the two-dimensional spin ½ XY model to see if this transition can also be described in the Kosterlitz-Thouless (KT) picture. Vortex and vortex-antivortex pair operators appropriate for this model on both the square and triangular lattices have been constructed. The expectation values of these operators in the ground state are obtained using the finite cell method of Oitmaa and Betts. This calculational method is described in some detail. The conclusion of this work is that although some vortices and antivortices are present in the ground state of the two-dimensional spin ½ XY model, it appears that all these excitations are paired and that no free vortices are present in this state. The interpretation of the results on the

triangular lattice is complicated by the relatively high density of vortices in the ground state on this lattice. These results are in agreement with the KT theory.

ACKNOWLEDGMENTS

First and foremost, let me acknowledge the moral and physical support that my parents have given me throughout my university career. I would also like to thank my sister, Chris, and her family for their help, especially in the early days of that career. The financial support of the National Research Council (now NSERC), in the form of a Postgraduate Scholarship, during the first two years of my graduate studies is gratefully acknowledged, as is the financial support of the Department of Physics for all three of my graduate years.

I would also like to mention the following people, to each of whom I owe a debt of gratitude for their concern and assistance at various stages of my association with the Physics department: Prof. D. Rankin, Prof. M. Razavy, and Prof. H. Umezawa. A special thanks must go to Prof. C.I.J.M. Stuart for his friendship and encouragement during particularly trying times.

With regard to the research presented in this thesis, my thanks go to Dr. Leo Marland and Dr. J. Oitmaa for the use of several computer programs they have written and for permission to quote the results of calculations which they have made. It is also a great pleasure to express my gratitude to Prof. D.D. Betts for suggesting the calculations described in this thesis and for his constant interest in the results of those calculations. Thanks must also go to Mrs. Lee Cech for her typing virtuosity.

It remains only to acknowledge the many conversations with my fellow students John Beamish, Dave Henty, Gordon Semenoff, Dave Spaner, Larry and Rick Sydora and John Whitehead, all of which were enjoyed, though only some had any connection with physics. A final thanks to J.E.R. for helping to make up my mind.

TABLE OF CONTENTS

CHAPTER		PAGE
I	INTRODUCTION	1
	A. Phase Transitions in Two-Dimensional Systems	1
	B. Vorticity Operators and Finite Cell Method	7
II	GROUND STATE PROPERTIES OF THE SPIN ½ XY MODEL	11
	A. Magnetization of the Ground State	11
	B. Cell Geometry and Symmetry Group	16
	C. Basis States	22
	D. Matrix Elements of the Hamiltonian and Ground State Energy	27
	E. Correlations	31
III	VORTICES IN THE GROUND STATE OF THE SPIN ½ XY MODEL	42
	A. Vortices	42
	B. Construction of the Vortex Operators	49
	C. Construction of the Vortex-Antivortex Pair Operators	56
	D. Presentation and Discussion of Results	62
IV	SUMMARY AND DISCUSSION	74
	A. Ground State Energy and Correlations	74
	B. Vortices and Free Vortices	77
	C. Experiments on Two-Dimensional Systems	82

* * *

BIBLIOGRAPHY	86
APPENDIX I - Two-spin Correlations in the Ground State of the XY Model in the Square Lattice. Finite Cell Results.	89
APPENDIX II - GXYSQDATA and GXY4COR	92
APPENDIX III - On the Ground State of the Antiferromagnetic Plane Rotator Model	95

LIST OF TABLES

TABLE	DESCRIPTION	PAGE
2.1	Ground state energy data for the spin ½ XY model on the square lattice.	23
2.2	Ground state correlations for the spin ½ XY model on the (a) square and (b) triangular lattices.	36
3.1	Vorticity and pair vorticity for the spin ½ XY model on the (a) square and (b) triangular lattices.	63
AI.1	Transverse and longitudinal correlations in the ground state of the spin ½ XY model on finite cells of the square lattice.	90

LIST OF FIGURES

FIGURE	DESCRIPTION	PAGE
2.1	Cell geometries on the square lattice.	18
2.2	Numbering of the nine-spin cell.	21
2.3	Sample symmetry operations on the nine-spin cell.	21
2.4	Basis states of the nine-spin cell and their symmetry numbers.	26
2.5	Ground state energy/spin ($-E_o/NJ$) for the spin ½ XY model on the square lattice as a function of 1/N.	32
2.6	Selected two spin correlations for the spin ½ XY model on the square and triangular lattices as functions of 1/N.	38
2.7	Selected four spin correlations for the spin ½ XY model on the square and triangular lattices as functions of 1/N.	39
3.1	Vortex configurations in a two-dimensional vector field.	44
3.2	Calculation of the vorticity of the plane rotator model, in the infinite temperature limit, on the square and triangular lattices.	46
3.3	Vortex states on the square lattice.	51
3.4	Vortex states on the triangular lattice.	53
3.5	Vortex-antivortex pair states on the triangular lattice.	58
3.6	Selected vortex-antivortex pair states on the square lattice.	61
3.7	Expectation values of vortex operators for the square and triangular lattices as functions of 1/N.	64
3.8	Expectation values of vortex-antivortex pair operators for the square and triangular lattices as functions of 1/N.	65

LIST OF FIGURES (CONT.)

FIGURE		PAGE
AIII.1	Triangular lattice partitioned into three geometrically similar sub-lattices.	99
AIII.2	Antiferromagnetic ground state of the plane rotator model on the triangular lattice.	99

CHAPTER I

INTRODUCTION

A. Phase Transitions in Two-Dimensional Systems

Convincing arguments exist to show that long-range order is not present at non-zero temperature for a wide variety of two-dimensional systems. As early as 1935, Peierls {1.1} argued that thermal motion of long-wavelength phonons would destroy the long-range order of a two-dimensional solid in the sense that the mean square deviation of an atom from its equilibrium position increases logarithmically with the size of the system, and the Bragg peaks of the diffraction pattern formed by the system are broad instead of sharp. Mermin showed later {1.2}, through the application of rigorous operator identities, that long-range order of this simple type is indeed absent. Application of similar arguments can be made to show that there is no spontaneous magnetization in a two-dimensional magnet with spins with more than one degree of freedom {1.3}. This latter condition allows for the well-known phase transition in the two-dimensional Ising model. It is also known {1.4} that the expectation value of the superfluid order parameter in a two dimensional Bose fluid is zero.

Contrasted with these results is persuasive evidence, from various sources, for some kind of phase transition in two dimensional systems. These sources include direct numerical work on a system of hard discs {1.5} and high temperature series expansions {1.6}, which predict a diverging susceptibility.

The evidence for such a transition is much stronger for the XY model than for the Heisenberg model{1.7}. While these results apply to the plane rotator model, which is equivalent to the S=∞ XY model, a phase transition is also believed to occur for the extreme quantum case, the spin ½ XY model {1.8}. If long range order as conventionally defined is not present at non-zero temperature, what is the nature of the predicted phase transition?

The physical picture which has emerged, largely in the works of Kosterlitz and Thouless {1.9}, is one in which "topological" excitations, in the form of vortices and antivortices for the plane rotator, play the primary role. This new type of long-range order, of a topological nature, may exist for a two-dimensional solid, neutral superfluid and for the XY model, but not for a superconductor or isotropic Heisenberg model. In the case of a two dimensional solid, the disappearance of topological long-range order is associated with a transition from an elastic to a fluid response to a small external shear stress.

The definition of long-range order which is adopted in this situation arises naturally from the dislocation theory of melting {1.10}, where it is supposed that a liquid close to its freezing point has a local structure similar to that of a solid. In the equilibrium configurations of the liquid, there is some concentration of dislocations which can move to the surface under the influence of an arbitrarily small shear stress and so produce viscous flow, while in the solid state

there are no free dislocations in equilibrium, and so the system is rigid. Now although isolated dislocations cannot occur at low temperatures in a large system, since their energy increases logarithmically with the size of the system, pairs of dislocations with equal and opposite Burgers vector have finite energy and are created by thermal excitation. These pairs can respond to an applied stress and so reduce the rigidity modulus. At sufficiently high temperatures, the largest pairs become unstable under an applied shear stress and produce a viscous response to the shear. The presence or absence of free dislocations can be identified then with the absence or presence of topological long-range order. It should be mentioned at this point that the theory of melting in such two-dimensional crystals and related problems of liquid-crystal phases in very thin films has been the subject of much recent activity {1.11}, {1.12}.

The topological excitation in the plane rotator model, or neutral superfluid, which is analogous to the dislocation in a two-dimensional crystal is the vortex. The plane rotator Hamiltonian is

$$H = -J \sum_{<i,j>} \vec{S}_i \cdot \vec{S}_j = -J \sum_{<i,j>} \cos(\phi_i - \phi_j) \quad , \qquad (1.1)$$

where $J>0$, $\| \vec{S}_i \| = 1$ and ϕ_i is the angle between $\vec{S}_i$ and some arbitrary reference direction. The symbol $<i,j>$ indicates that the sum is taken once over every bond pair (i,j). In the superfluid case, ϕ represents the phase of the complex

superfluid order parameter. By expanding the argument of the cosine function to order $(\phi_i-\phi_j)^2$ and taking a continuum limit it is possible to show {1.9} that the energy of an isolated vortex takes the form

$$E_v - E_o \simeq \pi J \ln (R/\delta) \quad , \tag{1.2}$$

where R is the size of the lattice, δ is the lattice spacing and E_o arises in the first term of the expansion of $\cos(\phi_i-\phi_j)$ and represents the energy of the zero temperature state of the plane rotator (see also {1.19}). Since isolated vortices (and antivortices) have a logarithmically divergent energy in the thermodynamic limit, $R/\delta \to \infty$, they cannot occur at very low temperatures. Now the entropy, S_v, associated with a free vortex is approximately

$$S_v \simeq 2k_B \ln(R/\delta) \quad , \tag{1.3}$$

which is arrived at by noting that the vortex center can occupy $N \simeq (R/\delta)^2$ lattice sites. Combining (1.2) and (1.3), the free energy associated with an isolated vortex, $F_v = (E_v-E_o) - TS_v$, can be written as

$$F_v \simeq (\pi J - 2k_B T) \ln(R/\delta) \quad , \tag{1.4}$$

and from this it can be seen that when the temperature is higher than

$$T_c \simeq \frac{\pi J}{2k_B} \quad , \tag{1.5}$$

the total free energy can be lowered by creating a vortex. In the theory of Kosterlitz and Thouless, the temperature T_c separates two distinct phases of the system. The "high" temperature phase, $T>T_c$, contains isolated vortices and antivortices, while below T_c there are no isolated vortices but closely bound vortex-antivortex pairs. The phase transition at T_c corresponds to the unbinding of these pairs and the creation of free or isolated vortices.

That the phase of the system at temperatures below T_c actually contains vortex-antivortex pairs follows from the result that such pairs have an attractive potential energy which cancels the logarithmic divergence (1.2) of a single vortex. This can be understood in terms of an analogy between the spin system containing a number of vortices and a two-dimensional plasma, originally made by Kosterlitz and Thouless {1.9, esp. (1973)}. If vorticity is identified with electric charge, vortices interact in the same way as two-dimensional electric charges, which, in turn, interact as parallel lines of charge in three dimensions. The interaction potential then depends logarithmically on the separation of the vortices. Just as, in two-dimensional electrostatics, a single charge has infinite electric field energy and a dipole (a pair of equal and opposite charges) has finite field energy, assuming the charges have finite size, so an isolated vortex has infinite energy, while a vortex-antivortex pair has finite energy. The vortex "dipoles" have a relatively short range effect on spin correlations compared with isolated

vortices (and antivortices) for the same reason that electric dipoles have short-range electric fields compared with those of isolated electric charges. Because of this the spin correlation function $\Gamma(\vec{r})$ has the same power law form, for $\|\vec{r}\|/\delta >> 1$, as predicted from spin-wave theory ignoring the effects of vortices, in the phase below T_c {1.13}. Once isolated vortices can appear, they have long range disordering effects on the spins and are expected to lead to an exponential decay of the correlation function $\Gamma(\vec{r})$, for large $\|\vec{r}\|/\delta$. The transition from one type of behaviour for $\Gamma(\vec{r})$ to the other indicates the existence of a phase transition.

All the above arguments can be made more quantitative, using renormalization group methods {1.14}. In particular, it is easy to see that the estimate (1.5) for the critical temperature is an upper bound. This critical temperature has been calculated as the temperature at which a pair of topological excitations will dissociate, ignoring the effect of other pairs in the system. These other pairs will relax in the field of the first pair, thereby renormalizing downward the e.g. rigidity modulus, in a two-dimensional crystal, and consequently reducing the critical temperature. This temperature is given {1.14} by the solution of the relation

$$\frac{\pi J}{2k_B T_c} - 1 = 2\pi \exp\left(-\frac{\pi^2 J}{2k_B T_c}\right) \quad . \tag{1.6}$$

Other predictions can be made of, for example, the critical exponent $\eta(T)$, of the spin correlation $\Gamma(\vec{r})$ for $T<T_c$ and

magnetic susceptibility, χ, in the magnetic realization of the planar model. This latter quantity is predicted to diverge as T approaches T_c from above and remains infinite for all $T<T_c$.

The significance of the Kosterlitz-Thouless picture is that it shows that a phase transition can be driven by the combining or breaking up of pairs of topological excitations without the appearance of conventional long range order like that of a ferromagnet. Similar topological arguments have attracted increasing attention in other areas of physics, notably the study of elementary particles where they may play a part in understanding the fundamental constituents of matter. With such an appealing view of the phase transition in the plane rotator model, it is natural to wonder whether these same considerations are applicable to the predicted phase transition in the spin ½ XY model.

B. Vorticity Operators and the Finite Cell Method

The aim of this thesis is to begin the investigation of the nature of the phase transition in the spin ½ XY model by examining the vorticity of the ground state of this model. The quantum nature of this model introduces complications in two areas. First, a notion of vorticity which is appropriate for quantum operators $\vec{S}_i$ must be established. This will be done by constructing an operator, v, among the eigenstates of which is included a vortex (and an antivortex) configuration. This operator will not commute with the

Hamiltonian of the model so the ground state will not be an eigenstate of this vorticity operator, but the expectation value of this operator in the ground state will provide an indication of the mean number of vortices, per lattice site, in this state.

The second problem arises because of the complex nature of the ground state of the spin ½ XY model. This state is not yet known exactly for the two-dimensional lattices which will be considered here, so it is necessary to use indirect means to determine the required ground state properties. The finite cell method, as outlined by Oitmaa and Betts {1.15}, will be employed in these calculations. The basis of this method is to calculate exactly the ground state and ground state spin correlations, for a sequence of small ($N \leq 19$) finite lattices of N spins and then extrapolate the results to the infinite lattice case. Such a procedure has been applied to the calculation of the ground state energy and transverse and longitudinal magnetizations of both the spin ½ XY magnet and the Heisenberg antiferromagnet on square and hexagonal lattices {1.15}. More recently calculations have been completed yielding the ground state energy, as a function of the anisotropy parameter, for the anisotropic Heisenberg antiferromagnet on the square lattice {1.16}. Both the ground state energy and transverse magnetization for the spin ½ XY magnet on the triangular lattice are now also known from such finite cell calculations {1.17}.

In the next chapter the finite cell calculations are described in some detail. The original results of Oitmaa and Betts (see also {1.18}), for the ground state energy of the spin ½ XY model on the square lattice, have been reproduced. While this result was obtained using a sequence of cells with an even number of spins, further calculations of this energy for several cells containing an odd number of spins are presented as well. In the third chapter, the concept of vorticity is introduced and quickly specialized to the case of a vector field defined on a lattice. The vortex operators for the square and triangular lattices are constructed, as are operators which are relevant to the study of vortex-antivortex bound pairs in the ground state of the spin ½ XY model. Once these operators are known, their expectation values can be expressed in terms of spin correlations available from Chapter II. These expectation values are presented and discussed in the last section of Chapter III. The final chapter presents a summary of the results obtained and further discussion on the implications of some of these results. Suggestions for further research are included here and the section ends with a brief discussion of experimental realizations of the ideas contained in this thesis. Three small appendices are included at the end of this thesis. The first is a compilation of two spin correlations for finite cells on the square lattice, while the second is a brief description of the contents of two computer files which were generated during the course of this work. The final appendix

contains a construction of the ground state of the antiferromagnetic planar model on the triangular lattice which was obtained following consideration of vorticity on the triangular lattice. As mentioned above, this thesis is but a part of the study of vortices in the spin ½ XY model. High temperature series expansions of the vortex and vortex-antivortex pair operators derived in chapter three are also being carried out. The complexity of such calculations however is restricting analysis to the triangular lattice at present. So although the applicability of finite cell calculations to this problem may be limited, it is certain that knowledge of the nature of the phase transition in the two-dimensional spin ½ XY model is only beginning to accumulate.

CHAPTER II

GROUND STATE PROPERTIES OF THE SPIN ½ XY MODEL

A. Magnetization of the Ground State

The problem to be examined in this chapter is that of determining several ground state properties of the spin ½ XY model, described by the Hamiltonian

$$H_{XY} = - 2J \sum_{<i,j>} (S_i^x S_j^x + S_i^y S_j^y) \qquad (2.1)$$

with $J>0$. The operators S_i^x, S_i^y are components of a spin ½ operator $\vec{S}_i$ associated with each lattice site i and the symbol $<i,j>$ indicates that the sum is taken over nearest neighbour pairs of sites on a regular two-dimensional lattice. The ground state energy $E_o \equiv <0|H_{XY}|0>$ will be the focus of this chapter but it is obvious that E_o is proportional to the nearest neighbour correlation, $E_o = - 2qNJ<0|S_o^x S_\delta^x|0>$, where δ is the lattice spacing and q the coordination number of the lattice. The calculational method can easily be extended to yield correlations between nth-nearest neighbour spin components.

Unlike, for example, the Ising model

$$H_I = - J \sum_{<i,j>} S_i^z S_j^z \quad , \qquad (2.2)$$

for which the ground state is clearly that in which the spins on all lattice sites are parallel, the ground state of H_{XY} cannot be written down by inspection and in fact is not

known exactly, in two or three dimensions. Rather than attempting an exact solution of the problem on an infinite lattice, the basic idea of the following calculations has been to carry out exact determinations of ground state energy (or correlations) for a sequence of small finite lattices of N spins and then to extropolate to the infinite lattice case. The N-spin cells are endowed with periodic boundary conditions so that an infinite lattice can be regarded as tiled with N-spin units. The limit $N \to \infty$ (or $N^{-1} \to 0$) then produces results appropriate for the infinite lattice "tiled" with a single unit.

For a finite spin ½ system it is in principle a straight forward matter to find the energy eigenvalues, the problem reducing to the diagonalization of the Hamiltonian in the 2^N dimensional space of states. Such a procedure becomes computationally intractable around N=8 unless symmetry considerations can be used to block diagonalize the Hamiltonian matrix. To this end consider the longitudinal magnetization operator

$$M_z = \sum_i S_i^z \quad , \tag{2.3}$$

which commutes with H_{XY} and thus provides a quantum number to label the eigenstates of the Hamiltonian. The following proof, due to Mattis {2.1}, shows that in the ground state Φ_o, the quantum number m_z is zero. It is first convenient to perform the rotation in spin space which takes S_i^y to S_i^z and S_i^z to $-S_i^y$, at all lattice sites i. Then the operators

H_{XY} and M_z have, in this new representation, the form

$$H_{XY} = -2J \sum_{<i,j>} (S_i^x S_j^x + S_i^z S_j^z) \quad , \tag{2.4}$$

and $$M_z = -\sum_i S_i^y = \tfrac{1}{2} i \sum_i (S_i^+ - S_i^-) \quad , \tag{2.5}$$

where the raising and lowering operators $S_i^{\pm}$ have been introduced according to the definitions

$$S_i^+ = S_i^x + iS_i^y$$

$$S_i^- = S_i^x - iS_i^y \quad . \tag{2.6}$$

Since the rotation in spin space is a similarity transformation, the eigenvalues of H_{XY} and M_z remain the same; in particular, the value of m_z when the energy is minimum will be unchanged by this transformation. The Hilbert space of states for a lattice with N sites consists of 2^N configurations of two distinct types:

$$\psi_{\alpha,ev.} = c_\alpha \prod_n (S_n^+)^{p_n} |0> \quad , \text{ with } \sum_n p_n = 0,2,4,\ldots, \tag{2.7a}$$

and $$\psi_{\alpha,od.} = c_\alpha \prod_n (S_n^+)^{p_n} |0> \quad , \text{ with } \sum_n p_n = 1,3,5,\ldots, \tag{2.7b}$$

where $|0>$ is the state with all spins "down", c_α is a normalization constant and the set of integers $\{p_n\}$ defines the state ψ_α. By using (2.6) for $S_i^x S_j^x$ in (2.4) it can be seen that H_{XY} has no matrix elements to connect the "even" and "odd" states. The two subspaces are decoupled and the ground state of each must be studied individually.

In the representation (2.4) and (2.5) the S_i^z are all diagonal, but the operators S_i^x are not. The ground state in either even or odd subspace takes the form

$$\Phi_{o,r} = \sum_\alpha F_\alpha^{(r)} \psi_{\alpha,r} \quad , \quad \text{with} \sum_\alpha |F_\alpha^{(r)}|^2 = 1 \quad , \qquad (2.8)$$

and, according to a well-known theorem of Frobenius {2.2}, has the property that all the $F_r^{(\alpha)}$, for r = even or odd, can be chosen real and positive. None of the $F_\alpha^{(r)}$ vanishes, since (2.4) connects all configurations within either subspace, nor is any $F_\alpha^{(r)}$ of opposite (negative) sign in the ground state. The proof of this statement is by contradiction. If some amplitude were not positive, the variational energy $\varepsilon_r^o = \langle \Phi_{o,r} | \mathcal{H}_{XY} | \Phi_{o,r} \rangle$ could be decreased by making it so. However, ε_r^o is already the lowest possible energy for the respective subspace, and hence all $F_\alpha^{(r)} > 0$. Finally, the ground state <u>in each subspace</u> is non-degenerate, as no other eigenstate of $\mathcal{H}_{XY}$ can satisfy the condition of having all positive amplitudes and yet be orthogonal to $\Phi_{o,r}$.

Consider first the state $\Phi_{o,even}$. Since M_Z as given by (2.5) connects the even and odd subspaces, and in fact takes even states into odd states, the only way $\Phi_{o,ev.}$ can be a simultaneous eigenstate of $\mathcal{H}_{XY}$ and M_Z is if

$$M_Z \Phi_{o,ev.} = 0 \quad . \qquad (2.9)$$

This argument also applies to $\Phi_{o,od.}$ so that the ground state magnetization of the XY magnet is zero. Thus, it suffices to examine the m_z=0 subspace of the 2^N dimensional Hilbert space of states.

Actually a complication arises if N, the number of sites per cell, is odd. In this case there is not state in either the even or odd subspace which has $m_z=0$, the minimum value of $|m_z|$ being $\frac{1}{2}$. By rotating (2.4) and (2.5) about the S_i^x axis in spin space such that $S_i^y \to -S_i^y$ and $S_i^z \to -S_i^z$, states in the even and odd subspaces are interchanged, M_Z is mapped into $-M_Z$ and H_{XY} is left invariant. This serves to illustrate an essential degeneracy of the two subspaces (even and odd) which is missing when N is an even integer. Because of this degeneracy, and unlike the even N situation, it is possible to have an eigenstate of H_{XY} which is some linear combination of eigenstates from both even and odd subspaces and which is also an eigenstate of M_Z, with non-zero eigenvalue.

The value of m_z in the odd N ground state is $\pm\frac{1}{2}$, depending on the chosen linear combination of $\Phi_{o,ev.}$ and $\Phi_{o,od.}$ To prove this rigorously consider a reference Hamiltonian

$$H^{ref.} = - 2J/N[(\Sigma_n S_n^x)^2 + (\Sigma_n S_n^z)^2] \qquad (2.10)$$

in which every spin on the same lattice as before interacts with every other spin. This is a molecular field limit of the Hamiltonian (2.4). On the one hand the ground states in the even and odd subspaces (2.7), $\Phi_{o,r}^{ref.}$ all have positive amplitudes, by Frobenius' theorem. They are therefore <u>not</u> orthogonal to their counterparts in Equation (2.8), and therefore share the same quantum number m_z. But now the energy levels of (2.10) are easily obtained (by back-rotating

$S_n^z \to S_n^y$) as $\varepsilon_{ref.} = -2J/N[I(I+1)-m_z^2]$ with $I=I_N$, I_N-1, $I_N-2,\ldots$, $m_z=I$, $I-1,\ldots,-I+1,-I$ and $I_N=N/2$. Evidently the ground states of $H_{ref.}$ belong to $I=I_N$ and $m_z=0$, when N is even, or $m_z=\pm\frac{1}{2}$ when N is odd.

To summarize the above arguments, it is sufficient to note that when considering the XY model on a lattice of N spin ½'s, one need only consider the $m_z=0$ subspace of the 2^N dimensional Hilbert space, when N is an even integer. When N is odd it is sufficient to consider either the $m_z=\frac{1}{2}$ or $m_z=-\frac{1}{2}$ subspaces. It should also be mentioned that these results apply in more generality than indicated by the above proof. For example, it can be seen that nothing requires all the spins to be equal and in fact the results above are easily generalizable to the case when the total spin on each site i is S_i, the place of N is taken by $2\Sigma_i S_i$. Further details and extensions are available in the original reference {2.1}.

B. Cell Geometry and Symmetry Group

The above effort has succeeded in reducing the number of states which must be considered in diagonalizing H_{XY} from 2^N to $N!/[(N/2)!]^2$, for N even or $N!/[(N+1/2)!(N-1)/2)!]$, for N odd. These latter are the numbers of states in the $m_z=0$ and $m_z=\frac{1}{2}$ subspaces respectively. For example, there are $N!/(N/2)!$ ways of placing N/2 objects ("up" spins) on N lattice sites; the extra factor (N/2)! corrects for the indistinguishability of the spins placed on the lattice. These numbers are still quite large. For N=16 there are

12,870 states in the $m_z=0$ subspace or $\sim$ 20% of the total 2^{16} states. A further reduction in the number of states which must be considered to diagonalize H_{XY} is needed to be able to push the calculation to cells with N>10. Such a reduction is afforded by consideration of the space group symmetry of the particular finite cell, since the ground state eigenvector must transform according to one of the irreducible representations of the space group. The same Frobenius theorem mentioned above requires the ground state eigenvector to transform according to the identity representation. That is, the ground state is invariant under the action of each element of the space group.

The determination of the space group relevant for each finite cell begins with the specification of the geometry of the cells upon which the calculation will be based. For the square lattice cells were chosen from two series: an even series, with cells of 4, 8, 10, 16 and 18 spins each, and an odd series, with cells of 4, 9 and 13 spins. These are shown in Figure 2.1. Although there are many possible choices for both the number of spins per cell and the geometry of a cell with a given number of spins, the choices made for this calculation are such that the symmetry group of each cell is as large as possible. All the cells considered here have a square border, a characteristic which increases the dimension of the point group (i.e. rotations and reflections) relative to that of cells with rectangular or rhomboidal boundaries. The number of spins which can be included in such square cells

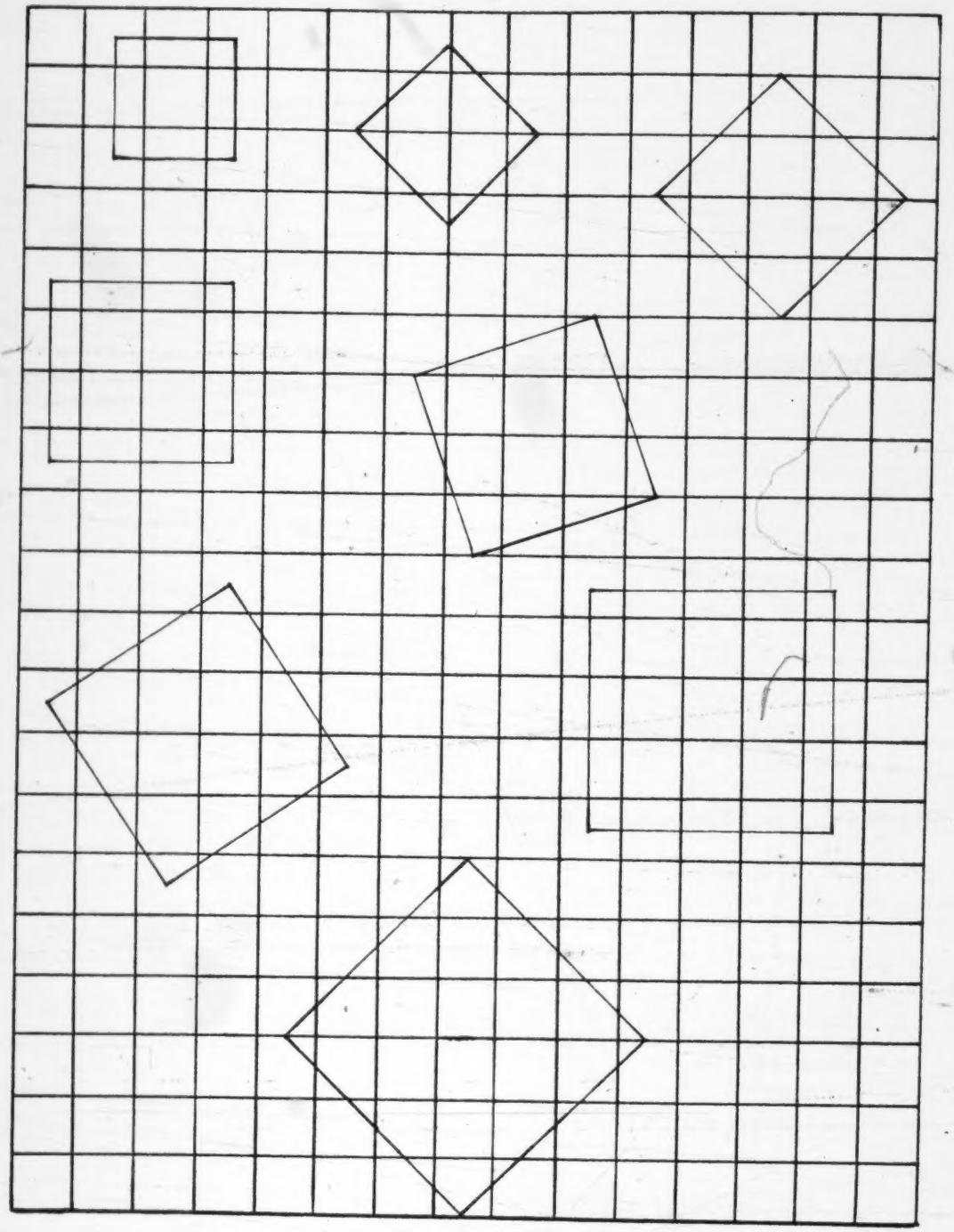

Figure 2.1 - Cell geometries on the square lattice.

is given by n^2+m^2, with n,m integer. The numbers n and m represent the coordinate distance between cell centers (i.e. 3 cells across, 1 cell up) and so $\sqrt{n^2+m^2}$ represents the distance between cell centers. This distance is also the length of an edge of the square boundary and so n^2+m^2 is both the area in units of δ^2, where δ is lattice spacing, of a cell and the number of spins, or lattice sites, the cell contains. This relation predicts an additional cell belonging to the odd series, with $N=17=(4)^2+(1)^2$, but calculations were not made for this value of N.

Once the cell geometry is chosen, an infinite lattice is tiled with N-spin cells and each cell is numbered, as shown for the 9-spin cell in Figure 2.2. Two groups are needed in order to be able to generate the full space group S_N. The first is the group of translations, T_N, which consist of those transformations on the tiled lattice which move each of the N spin sites to a given fixed site. These transformations can be visualized as moving the grid of cell boundaries over the underlying numbered lattice. The second is P_N, the group of point symmetries, consisting of rotations by 90°, denoted by C_4, $(C_4)^2$ and $(C_4)^3$, and reflections about vertical, horizontal and diagonal axis of the square cell. Some cells do not appear to be rotation symmetric, for example the N=8 and 10 cells. However, all cells do have this symmetry, although it may require a small shift of the boundary grid over the lattice to reproduce a similar pattern of spins in each cell. What is exceptional is that the N=10

and N=13 cells are not reflection symmetric, the point groups S_{10} and S_{13} consisting of only the proper rotations, including the identity.

Using the groups T_N and P_N as input, a computer program (GROUNDSYMM), available in the Statistical Physics Program and Data Library) was used to generate the group elements of S_N. The elements of these transformation groups are stored and manipulated as permutations of N numbers. For example, the identity element of S_9 is 1 2 3 4 5 6 7 8 9, which corresponds to sites on the 9-spin cell through the numbering illustrated in Figure 2.2. Four sample symmetry transformations are illustrated in Figure 2.3. Rotation about the center of symmetry by 270°, $(C_4)^3$, is represented as a permutation by 3 6 9 2 5 8 1 4 7, which means that under this transformation site 3 moves to site 1, site 6 moves to site 2, ..., etc. Also illustrated are the reflection about the 1-9 axis, σ_{d_1}, and a sample translation, t_3. With the symmetry transformations represented by permutations, the rules for multiplying permutations allow the quick calculation of such compound transformations as $(C_4)^3 \cdot t_3$:

(e	1 2 3 4 5 6 7 8 9)
t_3	3 1 2 6 4 5 9 7 8
$(C_4)^3$	3 6 9 2 5 8 1 4 7
$(C_4)^3 \cdot t_3$	2 5 8 1 4 7 3 6 9

Note that $(C_4)^3 \cdot t_3 \neq t_3 \cdot (C_4)^3$, and in general $p_i \cdot t_j \neq t_j \cdot p_i$,

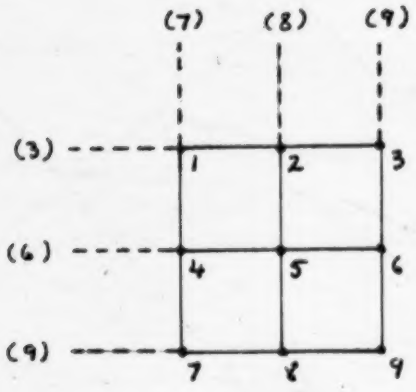

Figure 2.2 - Numbering of the 9-spin cell.

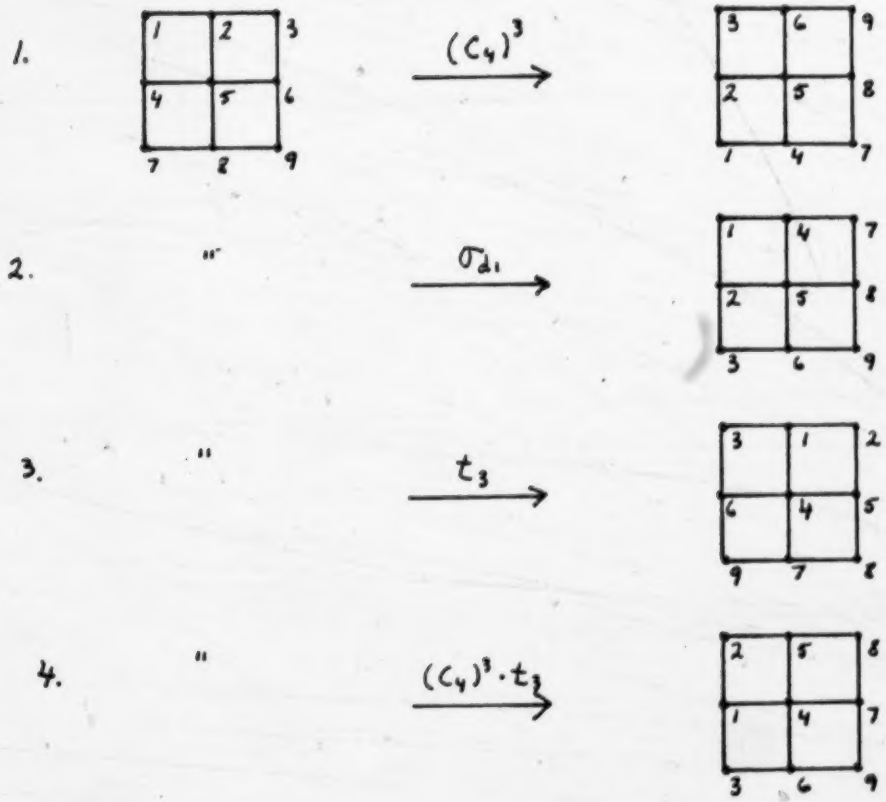

Figure 2.3 - Sample symmetry operations on the 9-spin cell.

$p_i \varepsilon P_N$, $t_j \varepsilon T_N$. Actually GROUNDSYMM does not simply calculate the product set $\{p_i \cdot t_j\}$. The program multiplies each element held in memory by every other such element and quits only when this procedure fails to generate a new symmetry transformation. The number of elements in each group S_N, for N>5, is shown in the second column of Table 2.1. It is interesting to note that in all cases the order of S_N, O(N), is simply the product of the orders of T_N and P_N: there are N translations, including the identity, for each N-spin cell while there are eight members of P_N (three rotations, four reflections and the identity) for N≠10 or 13. In these special cases P_N consists of just proper rotations (including the identity) thus has order 4. This result is true since the translation group T_N is a normal subgroup of S_N and so $S_N \equiv \{p_i \cdot t_j\} = \{t_b \cdot p_\ell\}$ and the order of S_N is the product of the orders of T_N and P_N. {2.3}.

C. Basis States

The ground state which is to be constructed from states in the m_z=0 subspace of the Hilbert space (2.7), symbolized as $H_o^{(N)}$, must be invariant under the action of the space group S_N. If this ground state, for each N-spin cell, is denoted by $\Phi_o^{(N)}$, the required invariance may be expressed as

$$g_i \Phi_o^{(N)} = \Phi_o^{(N)} \quad , \quad \text{for all } g_i \varepsilon S_N \quad . \tag{2.11}$$

If the members of the m_z=0 subspace of the Hilbert space of states are denoted by $\chi_\alpha^{(N)}$, then it is clear that if $\chi_\alpha^{(N)}$

Table 2.1 - Ground state energy data for the spin ½ XY model on the square lattice.

#of spins/cell N	order of S_N O(N)	#of basis states	$-E_o/J$	$-E_o/NJ$
4	-	2	5.6569	1.4142
8	64	6	9.3808	1.1726
10	40	9	11.5216	1.1522
16	128	153	17.9984	1.1249
18	144	398	20.1439	1.1191
5	-	1	6.0000	1.2000
9	72	5	10.3470	1.1497
13	52	38	14.6330	1.1256

enters into $\Phi_o^{(N)}$ with coefficient $a_\alpha^{(N)}$ so must each state $g_i\chi_\alpha^{(N)}$ for all $g_i \epsilon S_N$. But each $g_i\chi_\alpha^{(N)}$ is just one, though possibly the same, state $\chi_\beta^{(N)}$ in $H_o^{(N)}$. Only those states $\psi_\alpha^{(N)}$ in $H^{(N)}$ which are not related to each other by a symmetry transformation will enter into $\Phi_o^{(N)}$ with different coefficients $a_\alpha^{(N)}$. In this way such states are said to form an unsymmetrized basis for $\Phi_o^{(N)}$. The symmetrized basis for $\Phi_o^{(N)}$ is $\psi_{\alpha,sym.}^{(N)} = 1/n_\alpha^{(N)} \sum_i g_i\psi_\alpha^{(N)}$. The integer $n_\alpha^{(N)}$ is the number of group elements g_i which leave $\psi_\alpha^{(N)}$ invariant. Since there are $O(N)/n_\alpha^{(N)}$ distinct states $\chi_\beta^{(N)}$ generated by $\psi_\alpha^{(N)}$ and the sum above is taken over all O(N) group elements, the factor $1/n_\alpha^{(N)}$ is necessary to reproduce each $\chi_\beta^{(N)}$ exactly once.

To generate the basis states, use was made of the program GROUNDBASIS, also in the Statistical Physics Program and Data Library, modified of necessity for each size of cell. Taking the symmetry group S_N as well as one initial state $\psi_o^{(N)}$ and its symmetry number n_o as input, this program generates the complete set of basis states $\psi_\alpha^{(N)}$ and their symmetry numbers n_α. This is accomplished by first overturning nearest-neighbour pairs, with opposite spin, in order to generate a new state $\psi_1^{(N)}$ which is not related by symmetry transformation to $\psi_o^{(N)}$. More than one state inequivalent to $\psi_o^{(N)}$ may be generated by flipping just one pair of opposite spins; if so this state is also stored, along with its symmetry number. The program then moves on to $\psi_1^{(N)}$ and tries to generate new basis states by flipping nearest neighbour

pairs of opposite spin from this state. Eventually the point will be reached at which no new basis states are generated as these spin pairs are overturned. The program will keep trying to generate new states however, until a maximum number of spin pairs, relative to $\psi_o^{(N)}$, have been flipped. This number must be fed into the program through the input file. Experience has shown that all basis states will be generated if this number is $\gtrsim N/2$. For example, the last basis state of the 16 spin cell is generated after 6 pairs of spins have been flipped relative to the initial state. Execution stops once the maximum number of spin pairs have been overturned and the list of basis states, with their symmetry numbers and data concerning the numbers of spin pairs flipped is written into the output file.

The unsymmetrized basis elements for the 9-spin cell, along with their symmetry numbers,are presented in Figure 2.4. Actually, as mentioned above, these states are just the generators of the basis states, which can be written formally as the symmetrized sum

$$\psi_{\alpha,\text{sym.}}^{(N)} = \frac{1}{n_\alpha^{(N)}} \sum_{i=1}^{O(N)} g_i \, \psi_\alpha^{(N)} \quad . \tag{2.12}$$

In addition, we require the basis states to be normalized. Since there are $O(N)/n_\alpha^{(N)}$ distinct states in each symmetrized state $\psi_{\alpha,\text{sym.}}^{(N)}$, and because all the individual states in $H_o^{(N)}$ are normalized, the proper normalization factor is $(n_\alpha^{(N)}/O(N))^{\frac{1}{2}}$ and the symmetric, normalized basis states can be written as

$$\psi_0^{(9)} \simeq \begin{pmatrix} \bullet & \circ & \bullet \\ \circ & \bullet & \circ \\ \bullet & \circ & \bullet \end{pmatrix}, \quad n_0^{(9)} = 8$$

$$\psi_1^{(9)} \simeq \begin{pmatrix} \bullet & \bullet & \circ \\ \circ & \bullet & \circ \\ \bullet & \circ & \bullet \end{pmatrix}, \quad n_1^{(9)} = 2$$

$$\psi_2^{(9)} \simeq \begin{pmatrix} \bullet & \bullet & \bullet \\ \circ & \circ & \circ \\ \bullet & \circ & \bullet \end{pmatrix}, \quad n_2^{(9)} = 2$$

$$\psi_3^{(9)} \simeq \begin{pmatrix} \bullet & \bullet & \bullet \\ \circ & \bullet & \circ \\ \bullet & \circ & \circ \end{pmatrix}, \quad n_3^{(9)} = 2$$

$$\psi_4^{(9)} \simeq \begin{pmatrix} \bullet & \bullet & \bullet \\ \circ & \bullet & \circ \\ \circ & \bullet & \circ \end{pmatrix}, \quad n_4^{(9)} = 8$$

Figure 2.4 - Basis states of the 9-spin cell and their symmetry numbers. (=spin "up", .=spin "down")

$$\psi^{(N)}_{\alpha,\text{sym.,norm.}} \equiv \Psi^{(N)}_{\alpha} = \frac{1}{(n^{(N)}_{\alpha}\, O(N))^{\frac{1}{2}}} \sum_{i=1}^{O(N)} g_i \psi^{(N)}_{\alpha} \quad . \tag{2.13}$$

The number of symmetrized and normalized basis states $\Psi^{(N)}_{\alpha}$ for each N is shown in the third column of Table 2.1. Notice that this number grows rapidly with increasing N; this is to be expected since the number of states in $H^{(N)}_{o}$ is $(N!)/[(N/2)!]^2$, for even N, while the number of elements in S_N is proportional to N. As the number of basis states grows, so does the computing time necessary to generate them, and the limit of computational feasibility seems to reside at N=18 on the square lattice and N=19 on the triangular lattice. This latter cell has 838 basis states.

D. Matrix Elements of the Hamiltonian and Ground State Energy

Using the raising and lowering operators defined in (2.6), it is straightforward to recast the XY model Hamiltonian of (2.1) in the form

$$H_{XY} = -J \sum_{<i,j>} (S^{+}_{i}S^{-}_{j} + S^{+}_{j}S^{-}_{i}) \tag{2.14}$$

For a finite cell with periodic boundary conditions, every lattice site on the square lattice has four nearest neighbours. As an example, see Figure 2.2 where the dark lines are the structural links of the original cell and the dotted lines represent links due to the periodic boundary conditions. These can be thought of as "hooks" by means of which an infinite lattice is constructed with tiles of 9 spins each.

In the Hamiltonian (2.14) each nearest neighbour link is to be counted only once. The number of such distinct nearest neighbour links is 2N.

Thus for the 9 spin cell the Hamiltonian has eighteen terms and can be written in the following shorthand form:

$$-H_{XY}/J = (12)+(23)+(14)+(25)+(36)+(45)+(56)+(47)+(58) + (69)+(78)+(89)+(17)+(28)+(39)+(13)+(46)+(79), \tag{2.15}$$

where $(ij) = S_i^+S_j^- + S_i^-S_j^+$.

It is the matrix elements of the operator $-H_{XY}/J$, rather than H_{XY}, which are calculated by the program GROUNDXYHAM, the third and final member of the sequence available in the Statistical Physics Program and Data Library. This program also uses a standard diagonalization routine to yield the eigenvalues and eigenvectors of $-H_{XY}/J$ for all N≤16. For N=18 the iterative power method {2.4} must be used to generate the largest eigenvalue and corresponding eigenvector. This will be described subsequently.

For the moment consider an operator A, slightly more general than the Hamiltonian, in that it may consist of products of any number of spin operators on any combination of sites. The problem of evaluating the matrix elements of A in the basis $\psi_\alpha^{(N)}$ is that of evaluating expressions of the form

$$\langle\psi_\beta^{(N)}|A|\psi_\alpha^{(N)}\rangle = \frac{1}{(n_\alpha^{(N)} n_\beta^{(N)})^{\frac{1}{2}}} \left(\sum_j g_j \langle\psi_\beta^{(N)}|\right) \frac{1}{O(N)} \left(\sum_i A g_i |\psi_\alpha^{(N)}\rangle\right) . \tag{2.16}$$

Now the sum $\sum_j g_j \langle \psi_\beta^{(N)} |$ can be written as $(\sum_k g_k \langle \psi_\beta^{(N)} |) g_i^{-1}$ since in both cases the summation is over all elements $g \in S_N$. Then (2.16) becomes

$$\langle \psi_\beta^{(N)} | A | \psi_\alpha^{(N)} \rangle = \frac{1}{(n_\alpha^{(N)} n_\beta^{(N)})^{\frac{1}{2}}} (\sum_k g_k \langle \psi_\beta^{(N)} |) (\frac{1}{O(N)} \sum_i g_i^{-1} A g_i) | \psi_\alpha^{(N)} \rangle . \tag{2.17}$$

Specializing to the case of $-H_{XY}/J$, which is invariant under the action of S_N, equation (2.17) reduces to

$$\langle \psi_\beta^{(N)} | \frac{-H_{XY}}{J} | \psi_\alpha^{(N)} \rangle = \frac{1}{(n_\alpha^{(N)} n_\beta^{(N)})^{\frac{1}{2}}} (\sum_k g_k \langle \psi_\beta^{(N)} |) -\frac{H_{XY}}{J} | \psi_\alpha^{(N)} \rangle . \tag{2.18}$$

Operationally, equation (2.18) has the following meaning. The action of H_{XY} on the basis generator $\psi_\alpha^{(N)}$ is known from the action of the operators (ij); if the spins on sites i and j of $\psi_\alpha^{(N)}$ are different they are flipped and if these spins are the same the state is annihilated. What GROUNDXYHAM does is examine each element of the set $\{g_k \psi_\beta^{(N)}\}$ to find all the states which differ from $\psi_\alpha^{(N)}$ at two, and only two, lattice sites. This ensures that the two spins on these sites are different (one "up" and one "down"). The program subsequently checks the location of these two spins and counts each of those states for which the two differing spins are nearest neighbours. In this way the matrix element $(\sum_k g_k \langle \psi_\beta^{(N)} |) -\frac{H_{XY}}{J} | \psi_\alpha^{(N)} \rangle$ is generated for given α, β. This element is always an integer. To further reduce computing time only those $\beta \geq \alpha$, for a given α, need be considered as the operator $-H_{XY}/J$ is an observable and must have symmetric matrix

elements. The final step in the program is the multiplication of the raw matrix elements by the normalization factor $(n_\alpha^{(N)} n_\beta^{(N)})^{-\frac{1}{2}}$. The total set of matrix elements (2.18) is then stored awaiting the action of the diagonalization routine.

As mentioned above, a standard routine was used to calculate the complete set of eigenvalues and corresponding eigenvectors of the operator $-H_{XY}/J$ for $8 \leq N \leq 16$. The calculations for N=4 and 5 were completed "by hand". The resulting ground state energy $-E_o/J$ was obtained from the list of eigenvalues by inspection, and both $-E_o/J$ and $-E_o/NJ$ are tabulated in the last two columns of Table 2.1. For N=18, the matrix of $-H_{XY}/J$ is 398 by 398, which is above the limit of efficiency and accuracy of the standard diagonalization routines. Since only the largest eigenvalue and corresponding eigenvector are required, the iterative power method was used to generate these quantities. An initial normalized vector ϕ_o is chosen and the vector $\phi_o' = (-H_{XY}/J)\phi_o$ is calculated. This vector is in turn normalized, $\phi_1 = \phi_o'/\|\phi_o'\|$ and the procedure repeated with ϕ_1. After $n \simeq 25$ iterations, the vector ϕ_n has converged to the ground state eigenvector while $\| \phi_n' \|/\|\phi_n\|$ has converged to the maximum eigenvalue of $-H_{XY}/J$, i.e. $-E_o/J$. A suitable choice for the initial vector ϕ_o is one in which all entries are the same, i.e. 1, with an overall normalization factor of e.g. $(398)^{-\frac{1}{2}}$ in the case of the 18-spin cell Hamiltonian matrix. In this manner the eigenvalue $-E_o/J=20.1439$ was obtained.

Figure 2.5 is a graph of the ground state energy/spin, $-E_o/NJ$ vs. 1/N. The results for N an even integer lie on a straight line, while the odd N data do not lie on this line. Note however that a line drawn through the estimates for N=9 and 13 is parallel to the former line. The series corresponding to even N confirms the results of Oitmaa and Betts {2.5} and leads to a value of ground state energy/site, E_o/NJ, in the infinite lattice of -1.078±0.002. Although only two members of the odd N series are presented, since the results for N=5 do not lie on the line formed by the larger N data and in fact are not expected to, it would appear that the value of E_o/NJ predicted for the infinite lattice from the odd series, -1.07±0.01, is not consistent with the even N extrapolation. The larger uncertainty associated the odd N extrapolation reflects the use of only two data points and certainly before any definite conclusion can be reached, the ground state energy for the N=17 cell must be calculated. More will be said on this matter in Chapter IV - Summary and Discussion.

E. Correlations

Other quantities, besides the ground state energy, can be evaluated once the basis states have been computed. Principal among these quantities are two and four spin correlations, for example

$$\langle \phi_o^{(N)} | S_i^x S_j^x | \phi_o^{(N)} \rangle \quad , \tag{2.19}$$

$$\langle \phi_o^{(N)} | S_i^x S_j^x S_k^x S_l^x | \phi_o^{(N)} \rangle \quad , \tag{2.20}$$

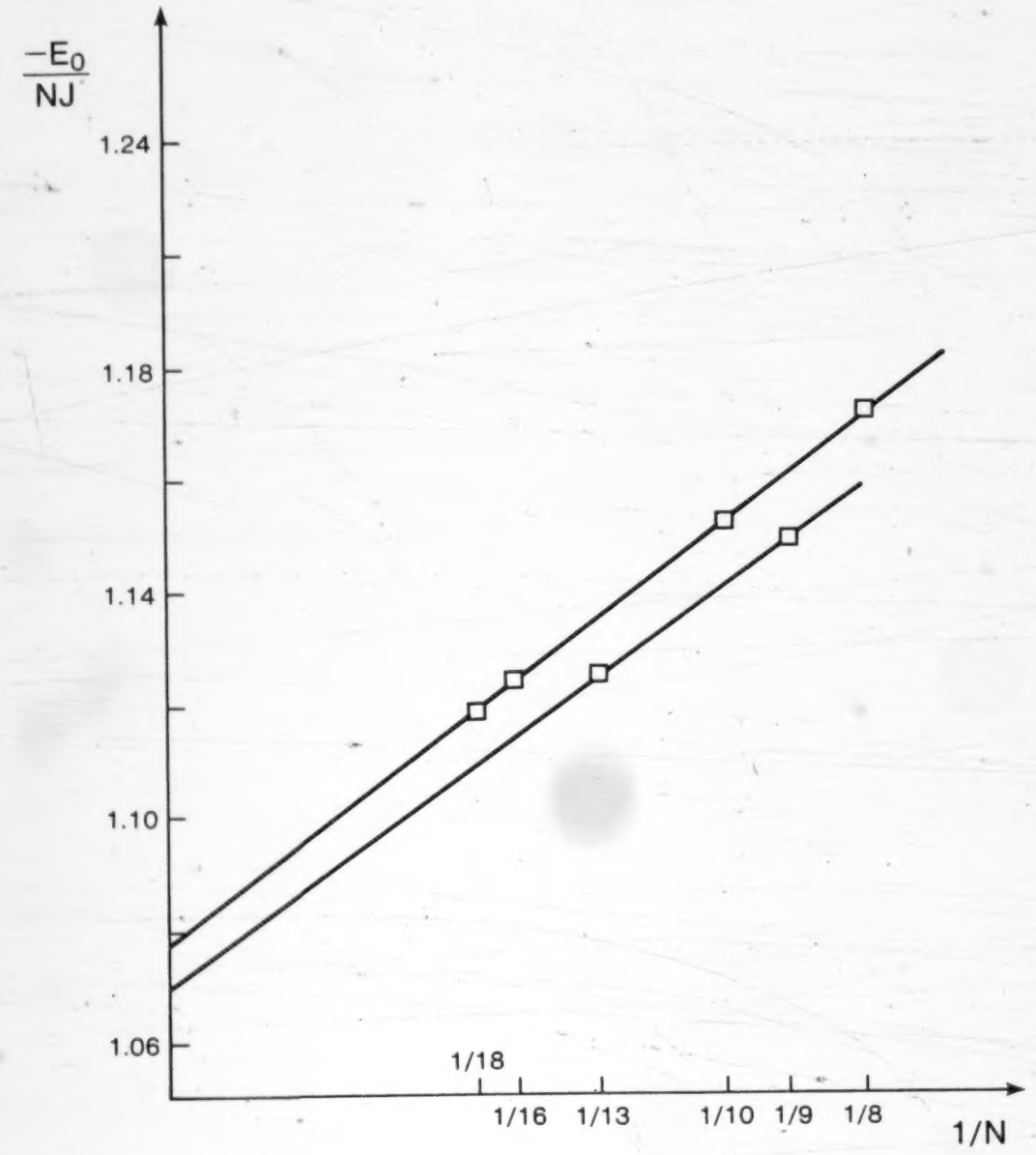

Figure 2.5 - Ground state energy/spin ($-E_0/NJ$) for the spin ½ XY model on the square lattice as a function of 1/N.

and

$$\langle\Phi_o^{(N)}|S_i^x S_j^x S_k^y S_l^y|\Phi_o^{(N)}\rangle \quad , \tag{2.21}$$

where the sites i,j,k and l may be chosen from any on the N-site cell. By translational invariance, the correlations depend only on the relative distance between these sites and not on their absolute location within the cell. For two spin correlations, this implies that there are only a few which are independent: nearest neighbour, second nearest neighbour,..., etc. The number of independent four spin correlations is greater and not as easily classified.

To evaluate correlations numerically, the operators S_i^x, S_i^y are expressed in terms of ladder operators $S_i^{\pm}$ through the definitions (2.6). The expressions are simplified by noting that the ground state $\Phi_o^{(N)}$ has $m_z=0$, so that the expectation value of operators of the form $S_i^+S_j^+$, $S_i^-S_j^-S_k^-$, $S_i^-S_j^-S_k^+S_l^-$, ..., etc. in this state is zero. Using this result, the correlations (2.19)-(2.21) become

$$\tfrac{1}{4}\langle\Phi_o^{(N)}|(i,j)|\Phi_o^{(N)}\rangle \quad , \tag{2.22}$$

$$\tfrac{1}{16}\langle\Phi_o^{(N)}|(il,jk) + (ik,jl) + (ij,kl)|\Phi_o^{(N)}\rangle \quad , \tag{2.23}$$

and

$$\tfrac{1}{16}\langle\Phi_o^{(N)}|(il,jk) + (ik,jl) - (ij,kl)|\Phi_o^{(N)}\rangle \quad , \tag{2.24}$$

where

$$(i,j) \equiv S_i^+S_j^- + S_i^-S_j^+ \quad , \tag{2.25}$$

and

$$(ij,kl) \equiv S_i^+S_j^+S_k^-S_l^- + S_i^-S_j^-S_k^+S_l^+ \quad . \tag{2.26}$$

The strategy for computing the correlations now follows from Equation (2.17), with the operator A identified with (i,j) in the case of two spin correlations and with (il,jk)+(ik,jl)±(ij,kl) for the four spin correlations (2.23) and (2.24). The procedure follows exactly that used to calculate the matrix elements of $-H_{XY}/J$, with the single exception that the states which are counted are not those which differ from $\psi_\alpha^{(N)}$ by two nearest-neighbour spins, but those which differ from $\psi_\alpha^{(N)}$ by a pair (or quadruplet) of spins in the set $\sum_i g_i^{-1} A g_i$, which is computed at the beginning of the program. A further complication in the evaluation of (2.24) is that the contribution from the states $(ij,kl)|\psi_\alpha^{(N)}\rangle$ must be counted with a negative sign, but this is easily accounted for. As the matrix elements $\langle\psi_\beta^{(N)}|A|\psi_\alpha^{(N)}\rangle$ are computed, the correlations (2.22)-(2.24) are generated using the expansion:

$$\langle\phi_o^{(N)}|A|\phi_o^{(N)}\rangle = \sum_\alpha a_\alpha^2 \langle\psi_\alpha^{(N)}|A|\psi_\alpha^{(N)}\rangle + 2 \sum_{\alpha,\beta>\alpha} a_\alpha a_\beta \langle\psi_\beta^{(N)}|A|\psi_\alpha^{(N)}\rangle \quad , \tag{2.27}$$

where the a_α are the coefficients of the ground state eigenvector:

$$\phi_o^{(N)} = \sum_\alpha a_\alpha \psi_\alpha^{(N)} \quad . \tag{2.28}$$

The details of the calculation of four spin correlations with the form (2.21) (or (2.24)) can be obtained from the program GXY4COR which has been placed in the Statistical Physics Program and Data Library.

As examples of the calculations described above, the two and four spin correlations which will be required in

Chapter III have been tabulated in Table 2.2. These correlations are expressed in terms of Pauli operators, $\vec{\sigma}_i$, which are related to the spin ½ operators by $\vec{S}_i = \frac{1}{2}\vec{\sigma}_i$, ($\hbar$=1), so that

$$\langle \sigma_i^x \sigma_j^x \rangle = 4\langle S_i^x S_j^x \rangle \quad , \tag{2.29}$$

and $$\langle \sigma_i^x \sigma_j^x \sigma_k^y \sigma_l^y \rangle = 16 \langle S_i^x S_j^x S_k^y S_l^y \rangle \quad , \tag{2.30}$$

and where of course the expectation value is taken in the ground state $\Phi_o^{(N)}$. If δ is the lattice spacing then second-nearest neighbour sites are $\sqrt{2}\delta$ units apart while third-nearest neighbours are 2δ units distant, on the square lattice. In Table 2.2(a), rows 1 and 2 represent respectively 2nd and 3rd nearest neighbour correlations. The four spin correlations involve sites lying on a "domino" formed by adjacent unit squares, or plaquettes. The exact geometry is not important here but will be discussed in the next chapter. The first two rows of Table 2.2(b) are nearest neighbour and second-nearest neighbour correlations on the triangular lattice while the four spin correlations are again taken over sites of a "domino" formed by two adjacent triangular plaquettes. Again, this will be made explicit in Chapter III. The two spin correlations were calculated by Dr. Leo Marland and obtained from him {2.6}, as was the data, e.g. basis states, ground state eigenvector, required to calculate the four spin correlations. It should be mentioned here, if it is not already apparent, that all the programs described above will work without modification for cells on the triangular

Table 2.2 - Ground state correlations for the spin ½ XY model on the (a) square and (b) triangular lattices.

(a)

N	8	10	16	18
1. $\langle\sigma_o^x\sigma^x_{\sqrt{2}\delta}\rangle$	0.52273	0.50746	0.48685	0.48797
2. $\langle\sigma_o^x\sigma^x_{2\delta}\rangle$	0.52273	0.50746	0.48685	0.47278
3. $\langle\sigma_1^x\sigma_5^x\sigma_4^y\sigma_6^y\rangle$	0.09091	0.09919	0.11278	0.08842
4. $\langle\sigma_1^x\sigma_3^x\sigma_2^y\sigma_4^y\rangle$	0.09091	0.07222	0.04843	0.05299
5. $\langle\sigma_1^x\sigma_3^x\sigma_2^y\sigma_6^y\rangle$	0.09091	0.09919	0.07997	0.08264
6. $\langle\sigma_1^x\sigma_3^x\sigma_4^y\sigma_6^y\rangle$	0.09091	0.09919	0.07997	0.06909

(b)

N	7	9	13	19
1. $\langle\sigma_o^x\sigma^x_{\delta}\rangle$	0.57143	0.56103	0.55052	0.54391
2. $\langle\sigma_o^x\sigma^x_{\sqrt{3}\delta}\rangle$	-	0.52111	0.50295	0.48914
3. $\langle\sigma_1^x\sigma_2^x\sigma_3^x\sigma_4^x\rangle$	-	0.47837	0.45715	-
4. $\langle\sigma_2^x\sigma_4^x\sigma_1^y\sigma_3^y\rangle$	-	0.13100	0.11796	-

lattice. All that is needed to prime the sequence is a choice of finite cell and the elements of the symmetry groups T_N and P_N expressed as permutations.

Figures 2.6 and 2.7 are respectively graphs of the two spin and four spin correlations, for both lattices, as functions of 1/N. The two spin correlations on the triangular lattice are well behaved, with the second-nearest neighbour correlation forming a near perfect straight line. There is a slight deviation of the nearest neighbour correlation at N=19 which, since the ground state energy is proportional to the nearest-neighbour correlation, is also evident in the former quantity and is of unknown origin {1.17}. A rather surprising feature of the square lattice data is that both second and third-nearest neighbour correlations are equal for $N \leq 16$. This degeneracy is absent in the results from the 18-spin cell calculation, which is to be expected as these correlations are certainly not the same in the infinite lattice limit. This phenomenon may be due to some unaccounted symmetry of the $N \leq 16$ cells, but whatever its cause, it is clear that extrapolation to the infinite lattice will be inaccurate if this is based on either all data points or simply the results for $N > 16$. When the four spin correlations are examined, the situation appears much worse, for the square lattice at least. Degeneracy is evident again: for N=8, all four of the four spin correlations are equal, for N=10 three of them are the same while at N=16 two of them are the same, and it is not until N=18 that the four correlations are all

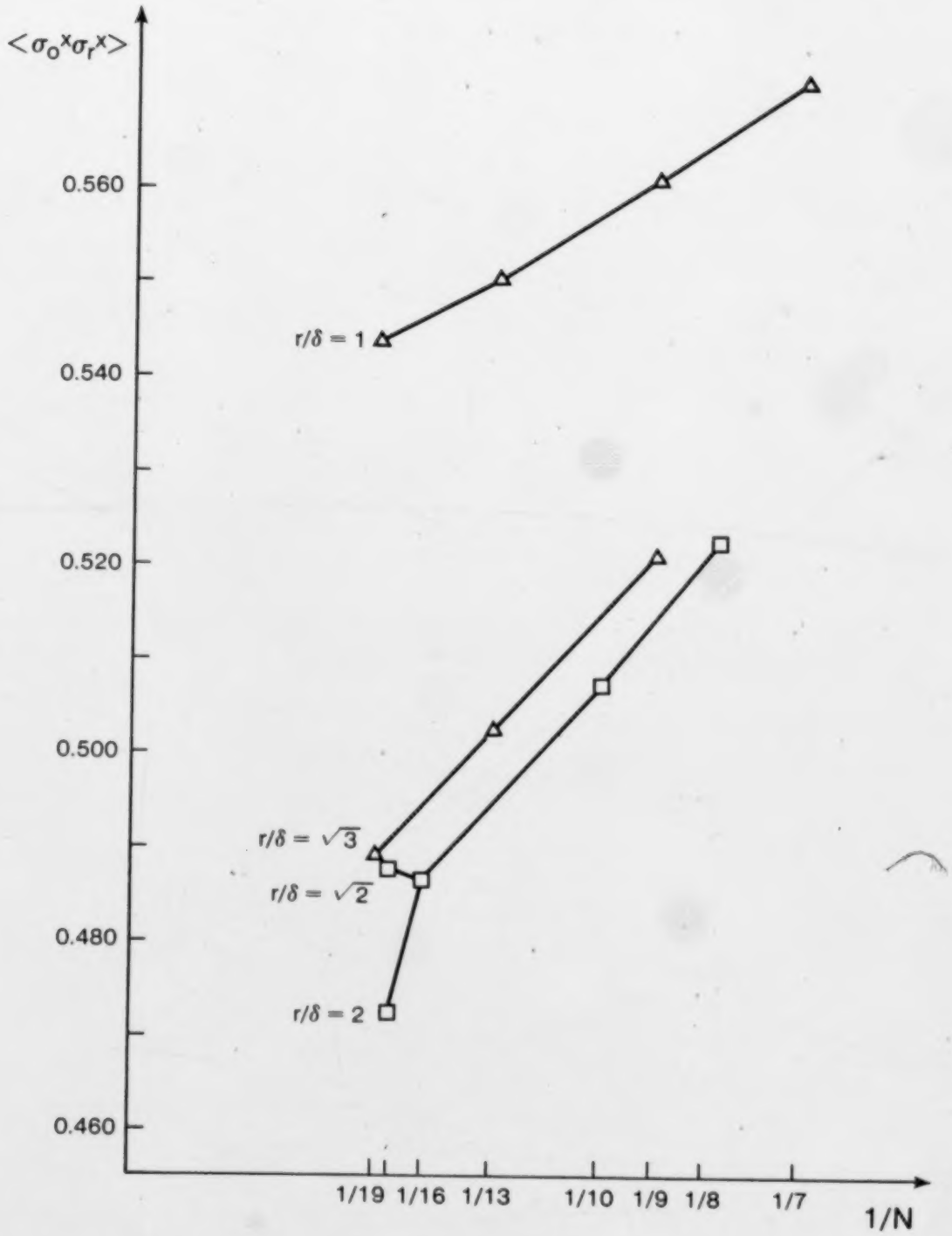

Figure 2.6 - Selected two spin correlations for the spin ½ XY model on the square (squares) and triangular (triangles) lattices as functions of 1/N.

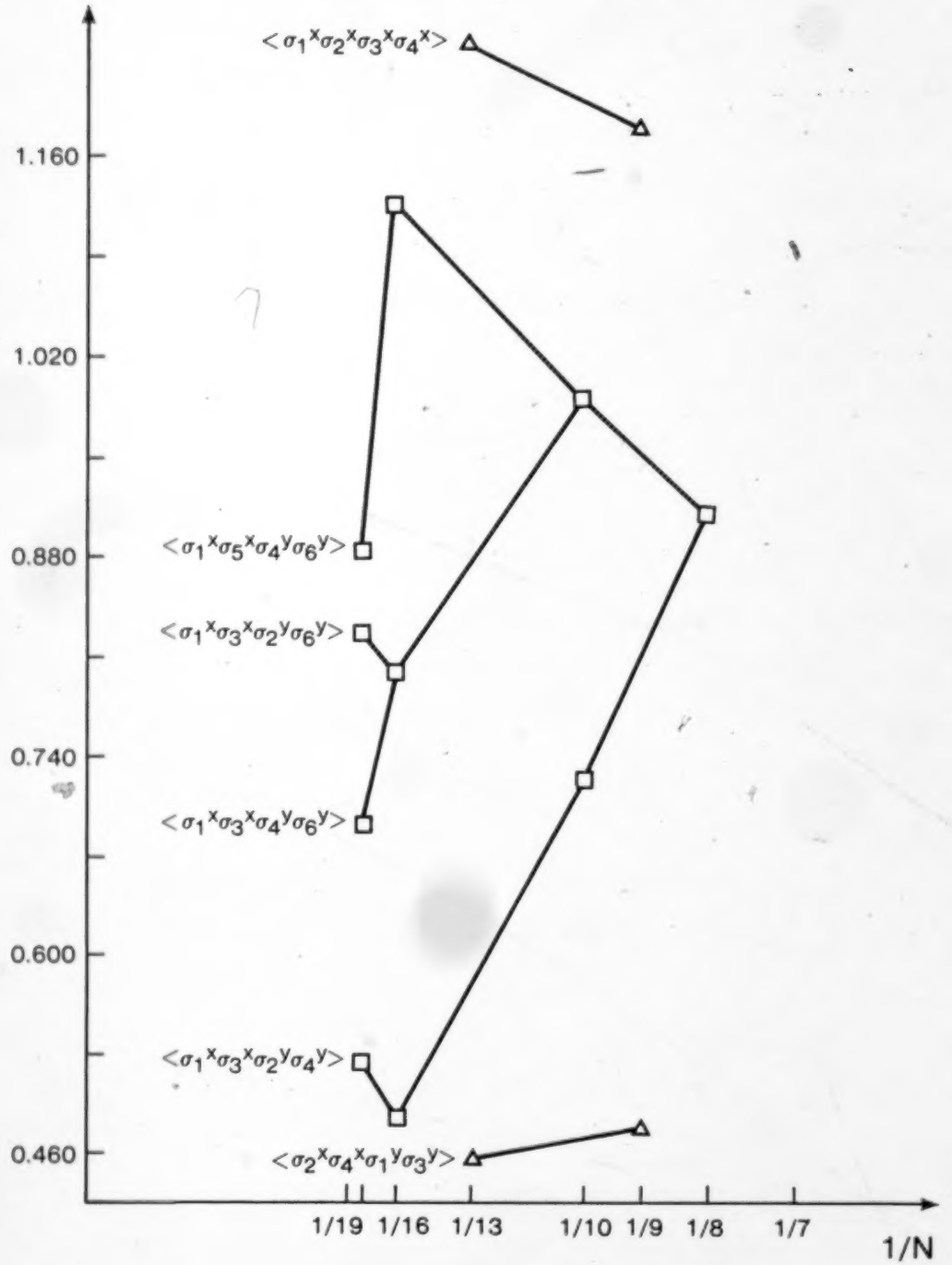

Figure 2.7 - Selected four spin correlations for the spin ½ XY model on the square (squares) and triangular (triangles) lattices as functions of 1/N; (see Figures 3.5 and 3.6 for a definition of the coordinates).

distinct. Aside from this however, and perhaps acting as a cause for some of the degeneracy, is the fact that for N<10, the area of the cell is of the same order as the area over which the four site correlations are evaluated. For the same reason that the ground state energy per spin calculated for N=4 (and 5) does not lie on the straight line formed by the larger N results, so to it is expected that the four spin correlations for N=8 and 10 will likely not lie on a line with larger N data. All the spins of cells with a small number of sites are too highly correlated, because of the periodic boundary conditions, to accurately reflect the situation in the infinite lattice over distances greater than ~ half the cell's linear dimension. With this criterion the four spin correlation for the 16 spin cell is just within the limit of applicability, although too much trust should not be placed in results for N>16. For example both the correlations $\langle\sigma_1^x\sigma_3^x\sigma_4^y\sigma_6^y\rangle$ and $\langle\sigma_1^x\sigma_4^x\sigma_5^y\sigma_6^y\rangle$ extrapolate to negative numbers using only the data points N=16 and N=18! Although only two data points are available for the four spin correlations on the triangular lattice, there is reason to believe that an extropolation to the infinite lattice based on these two points alone would be sufficiently accurate. First, the two spin correlations, particularly the second-nearest neighbour correlation, are well behaved, showing no degeneracy which would "artificially" shift some data points. Second, the area over which the four site correlation is taken is not large with respect to cell size, even at N=9, for which the

ratio of these two areas is roughly comparable with that for N=16 on the square lattice. The maximum distance between points on one triangular "domino" is $\sqrt{3}\delta$, compared with a maximum separation of $\sqrt{5/2}\delta$ for points of the "domino" on the square lattice. Although the four spin correlations for N=19 should be calculated, it is to be expected that they will lie close to the lines formed by the data points already known and plotted in Figure 2.7.

CHAPTER III

VORTICES IN THE GROUND STATE OF THE SPIN ½ XY MODEL

A. Vortices

Let $\vec{u}(x,y,z)$ be a vector field, or flow, defined on a three-dimensional Cartesian space. The vorticity of this flow, $\vec{\omega}$, is defined by $\vec{\omega}$=curl $\vec{u}$. The usefulness of this quantity in understanding flow configurations derives in great part from the fact that vorticity corresponds to a rotation of the vector field. This follows from the definition of curl as

$$\hat{n}\cdot\text{curl}\ \vec{u} = \lim_{s\to 0} \frac{1}{S} \oint \vec{u}\cdot d\vec{l} \quad , \tag{3.1}$$

where $\hat{n}$ is the unit vector normal to the surface S, around the edge of which the line integral is taken. In contrast with this it is possible to make the definition adopted in this work: a configuration is said to possess unit vorticity (antivorticity) about a selected point if on traversing a contour about that point in a positive direction the vector field makes a complete (2π rad.) turn in the same (opposite) direction. It is clear that this definition is appropriate only for fields restricted to a plane. Illustrations of this definition are presented in Figure 3.1. The set of flow configurations which possess vorticity $\vec{\omega}$ is not the same as the set of configurations which possess vorticity according to the second definition. It is possible to exhibit flows which possess vorticity according to either definition, both definitions or, of course, which do not have any vorticity at all. For example, it is clear that

the first of Figure 3.1a) is such that $\vec{\omega}=0$ at every point while $\vec{\omega}\neq 0$ in general for the second configuration. This illustrates one of the most useful properties of the operational definition, namely that a vortex (or antivortex) remains so if the vector field $\vec{u}(x,y)$ is subject to rotation by a fixed amount at each point (x,y). The vorticity $\vec{\omega}$ does not share this invariance.

Consider now the plane rotator model, defined by the Hamiltonian

$$H_{PR} = -J \sum_{<i,j>} \vec{S}_i \cdot \vec{S}_j = -J \sum_{<i,j>} \cos(\phi_i - \phi_j) \qquad (3.2)$$

where $\| \vec{S}_i \| = 1$ and ϕ_i is the angle $\vec{S}_i$ makes with some arbitrary axis, $0 \leq \phi_i \leq 2\pi$. This model is the classical analogue of the spin ½ XY model and is in fact the same obtained from the spin s XY model in the limit as $s \to \infty$. To help illustrate the concept of vorticity before proceeding to a discussion of vortices in the spin ½ XY model, it will be shown below that the probability of finding a vortex (or an antivortex) about any given location in the square lattice, in the limit of infinite temperature, is 0.167. It should be mentioned here that consideration of a vector field, $\vec{S}_i$, defined on a lattice does not interfere with the definition of vorticity adopted above. The effect of the lattice is to introduce a contour

(a) unit vortices

(b) unit antivortices

Figure 3.1 - Vortex configurations in a two-dimensional vector field.

of minimum size which, on the square lattice, is just a square with an edge of length δ and vertices formed by lattice sites. It is about this contour, known as a plaquette, that vorticity will be calculated.

In the limit of infinite temperature, the probability of finding the angle of the spin $\vec{S}_i$, with respect to some fixed axis, lying in the range θ to $\theta + d\theta$ is just $d\theta/2\pi$, independent of the orientation of any other spin on the lattice. The problem of finding the probability of a vortex configuration then reduces to that of finding the proportion of all spin configurations on a plaquette which are vortices. Further, because a vortex is invariant under a rotation of all spins by a fixed amount, it is only necessary to consider the orientation of three spins relative to that of the fourth, which can be assumed fixed. This fixed spin will be placed on site 1, and the positive direction along the plaquette will be chosen to coincide with the direction 1 2 3 4. The spin on site 3 will be placed at angle of θ with respect to the axis defined by the spin on site 1. Two cases will be distinguished: $0 \leq \theta \leq \pi$, illustrated by Figure 3.2(a) and $\pi \leq \theta < 2\pi$, illustrated by Figure 3.2(b). Once the spins at sites 1 and 3 are fixed, the question becomes the determination of the orientations of the spins on sites 2 and 4 which will yield a vortex configuration. Consider first Figure 3.2(a). The spin on site 2 may lie anywhere in the hatched region, including the axis, while the spin on site 4 may lie in the hatched region about this site, that is at an angle $\pi < \phi < \pi + \theta$

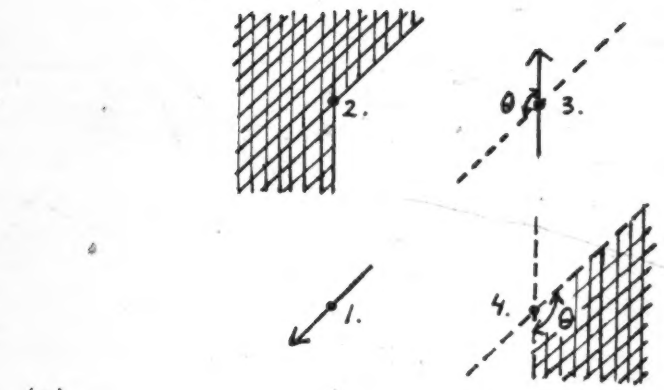

(a)

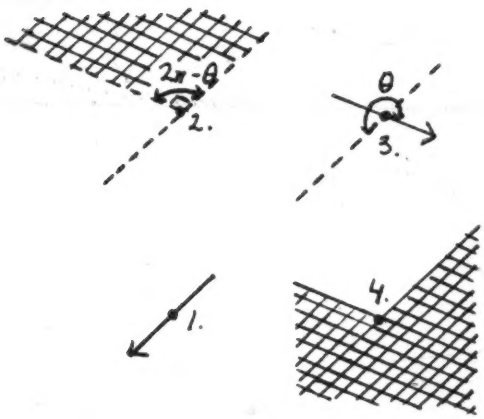

(b)

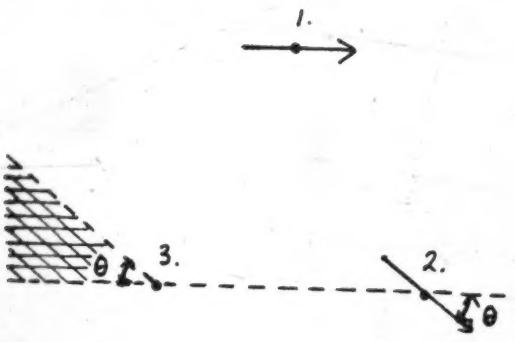

(c)

Figure 3.2 - Calculation of the vorticity of the plane rotator model, in the infinite temperature limit, on the square (a), (b) and triangular (c) lattices.

with respect to the axis defined by spin 1. These hatched regions are constructed so that no spin lying inside these regions is more than $+\pi$ rad. "away" from the axes defined by both the spins on site 1 and site 3. This ensures the spins make a positive turn on going around the plaquette in a positive direction. Note that the results imply that no vortex can be formed when both spin 1 and spin 3 are parallel ($\theta=0$). The proportion of all spin configurations which are vortices when spin 3 lies in the range θ to $\theta+d\theta$, with $0\leq\theta\leq\pi$, is then

$$dP^{(a)} = \underbrace{\frac{\theta}{2\pi}}_{4} \cdot \underbrace{\frac{d\theta}{2\pi}}_{3} \cdot \underbrace{\frac{(2\pi-\theta)}{2\pi}}_{2} \qquad (3.3)$$

Similarily, the proportion of all configurations which are vortices when spin 3 lies in the range θ to $\theta+d\theta$, with $\pi\leq\theta\leq2\pi$, is, from Figure 3.2(b),

$$dP^{(b)} = \underbrace{\frac{(2\pi-\theta)}{2\pi}}_{2} \cdot \underbrace{\frac{d\theta}{2\pi}}_{3} \cdot \underbrace{\frac{\theta}{2\pi}}_{4} \quad . \qquad (3.4)$$

It follows from previous remarks that the probability of finding a vortex on a given plaquette, in the infinite temperature limit is

$$P_v = \int_0^{\pi} dP^{(a)} + \int_{\pi}^{2\pi} dP^{(b)}$$

$$= \frac{1}{8\pi^3} \cdot \int_0^{2\pi} \theta(2\pi-\theta)\,d\theta$$

$$= 0.167 \quad . \tag{3.5}$$

The probability of finding an antivortex on a given plaquette is also found to be 0.167, a result which follows immediately from the above arguments once it is noted that an antivortex can always be formed from a vortex by inverting two diagonally opposite spins, e.g., the spins on sites 1 and 3. The probability of finding either a vortex or an antivortex in the infinite temperature limit of the plane rotator model is then 0.333.

The same type of calculation can be carried out for the plane rotator on the triangular lattice, for which the basic plaquette is a triangle of side δ with vertices formed by lattice sites. Figure 3.2(c) illustrates the situation in this case. Positive direction around the plaquette is taken as 1 2 3. The fixed spin is placed on site 1 and the spin on site 2 is oriented at an angle of θ, $0 \leq \theta \leq \pi$, with respect to the axis defined by the fixed spin. Note that for the triangular lattice vortex configurations correspond to $0 \leq \theta \leq \pi$ while antivortex configurations are formed for $\pi \leq \theta < 2\pi$. Referring to Figure 3.2(c), the differential probability of finding a vortex on a given plaquette is

$$dP^{(c)} = \underbrace{\frac{\delta}{2\pi}}_{3} \cdot \underbrace{\frac{d\theta}{2\pi}}_{2} \quad , \tag{3.6}$$

sites:

so that the total probability is

$$P_v = \int_0^{\pi} dP^{(c)}$$

$$= \frac{1}{4\pi^2} \int_0^{\pi} \theta d\theta$$

$$= 0.125 \quad , \tag{3.7}$$

as in the case of the square lattice. The probability of finding an antivortex is then 0.125, so that the total probability of finding a vortex or an antivortex on the triangular lattice is 0.250.

B. Construction of the Vortex Operators

In the previous section the concept of vorticity was introduced and, almost immediately, adopted from vector fields defined on a continuous space to those defined on a two-dimensional lattice. One further modification must be introduced before vortices in the ground state of the spin ½ XY model can be discussed, and this is the quantization of the vector field, $\vec{S}_i$. The considerations outlined above were appropriate for a classical field $\vec{S}_i$ which could assume any in a continuous range of orientations. In the spin ½ XY model, $\vec{S}_i$ becomes a quantum mechanical, spin ½ operator; what becomes of the vorticity?

The answer to this question adopted in this work is to construct an operator, the vorticity operator v, the eigenstates of which are a vortex or an antivortex configuration, or neither, over a basic plaquette. The corresponding

eigenvalues will be +1, -1 and 0 respectively. The expectation value of this operator in the ground state of the spin ½ XY model will then be interpreted as representing the mean number of vortices per site present in this state.

To construct the vorticity operator appropriate for the square lattice, consider first the basic plaquette shown in Figure 3.3. The spins on sites 1 and 3 are quantized along the x axis while the spins on sites 2 and 4 are quantized along the y axis. The individual site operators are Pauli operators $\vec{\sigma}$, and so there are a total of 16 distinct states possible on each plaquette. Since the vorticity is invariant under a spin flip applied to all sites, only 8 of these states will contribute independently to the construction of v. These 8 states are shown in Figure 3.3. Of these 8 states, only state 1 represents a vortex while only state 7 represents an antivortex; all others show no vorticity and so v applied to these states must be zero. The next step is to pick out eight functions of the four spin variables $\sigma_1^x, \sigma_2^y, \sigma_3^x$, and σ_4^y from which to construct an operator v which gives +1 when applied to state 1, -1 when applied to state 7 and annihilates all the other states. These functions must be even functions of the basic operators, a suitable choice being $\sigma_1^x\sigma_2^y, \sigma_1^x\sigma_4^y$, $\sigma_2^y\sigma_3^x$, $\sigma_3^x\sigma_4^y$, $\sigma_1^x\sigma_3^x$, $\sigma_2^y\sigma_4^y$, $\sigma_1^x\sigma_2^y\sigma_3^x\sigma_4^y$ and 1. The final task is to solve the 8 equations for the coefficients of these operators in the expansion of v obtained from each of the 8 states in Figure 3.3. Passing over the details of this step, it is found that only four of the above operators are needed

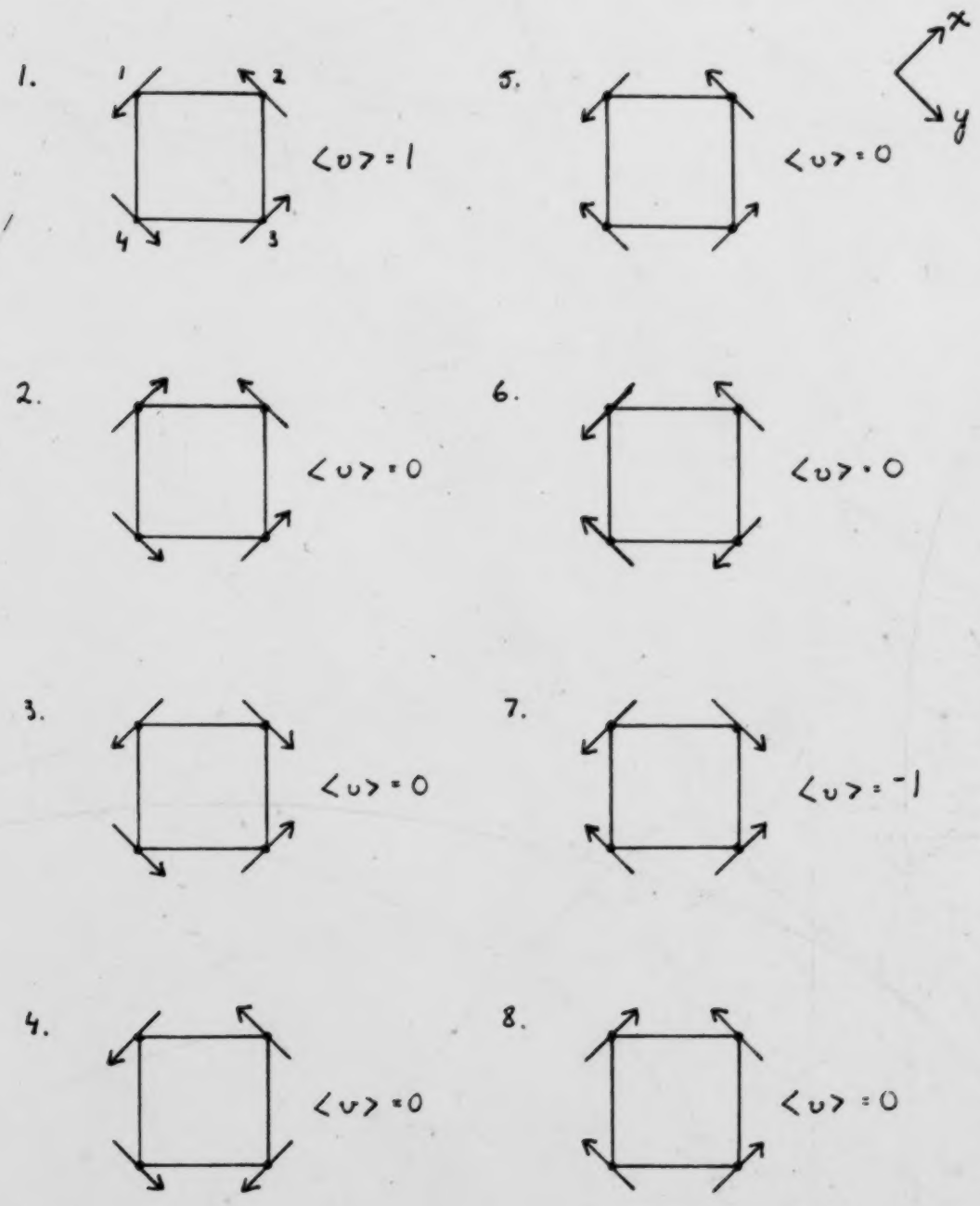

Figure 3.3 - Vortex states on the square lattice.

to describe v, which can then be written as

$$v = \frac{1}{4}(\sigma_1^x\sigma_2^y - \sigma_1^x\sigma_4^y + \sigma_3^x\sigma_4^y - \sigma_2^y\sigma_3^x) \quad . \tag{3.8}$$

When the expectation of this operator is taken for the spin ½ XY model however, it is found that $\langle v\rangle=0$, at any temperature, since $\langle\sigma_i^x\sigma_j^y\rangle=0$ by symmetry, for any sites i,j on the lattice. The interpretation of this result is that in the ground state the number of vortices and antivortices is equal. To circumvent this result the operator v is squared and the subsequent expectation value interpreted as the (mean) total number of vortices and antivortices per site in the ground state. Carrying out this operation yields

$$v^2 = \frac{1}{4}(1 - \sigma_2^y\sigma_4^y - \sigma_1^x\sigma_3^x + \sigma_1^x\sigma_2^y\sigma_3^x\sigma_4^y) \quad , \tag{3.9}$$

so that

$$\langle v^2\rangle = \frac{1}{4}(1 - 2\langle\sigma_o^x\sigma_{\sqrt{2}\delta}^x\rangle + \langle\sigma_1^x\sigma_3^x\sigma_2^y\sigma_4^y\rangle) \quad , \tag{3.10}$$

where the equality $\langle\sigma_1^x\sigma_3^x\rangle=\langle\sigma_2^y\sigma_4^y\rangle$ holds, at any temperature, in the XY model due to the symmetry of x and y in H_{XY}, and $\langle\sigma_1^x\sigma_3^x\sigma_2^y\sigma_4^y\rangle=\langle\sigma_1^x\sigma_2^y\sigma_3^x\sigma_4^y\rangle$ since the operators at different sites commute.

The operator v' appropriate for the triangular lattice can be constructed in a similar manner. In Figure 3.4(a) the possible states on a triangular plaquette are illustrated. The spin-flip states are again not necessary. On this lattice it is necessary to choose the direction of quantization of $\vec{\sigma}_2$ to be the v-direction and that of $\vec{\sigma}_3$ to be the u-direction.

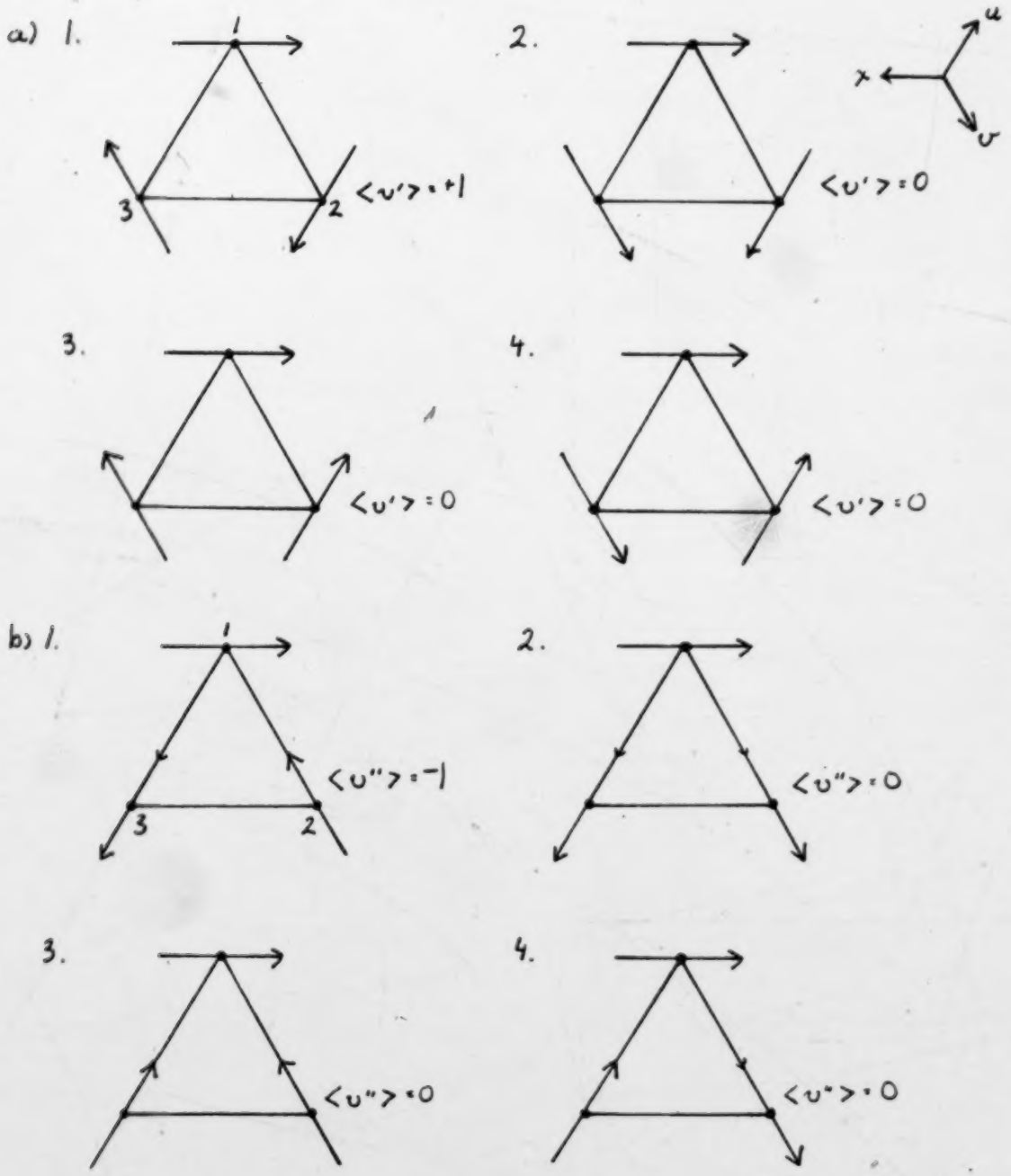

Figure 3.4 - Vortex states on the triangular lattice.

Neither of these are orthogonal to x or y, and in fact the quantities σ^u and σ^v can be written in components as

$$\sigma^u = \sqrt{3}/2\ \sigma^y - \frac{1}{2}\sigma^x \quad , \tag{3.11a}$$

$$\sigma^v = -\sqrt{3}/2\ \sigma^y - \frac{1}{2}\sigma^x \quad . \tag{3.11b}$$

The first state, for which $\langle v' \rangle = 1$, has all three spins oriented in the positive coordinate directions while the other three have at least one spin oriented in the negative coordinate direction. The operator v' can thus be written down immediately as

$$v' = \frac{1}{4}(1 + \sigma_1^x\sigma_3^u + \sigma_1^x\sigma_2^v + \sigma_2^v\sigma_3^u) \quad . \tag{3.12}$$

This operator has the interesting properties that $v' = (v')^2$ and $\langle v' \rangle \neq 0$. The former can be shown by direct computation while the latter can be seen in the following manner. Using the relations (3.9), the identities $\langle \sigma^x\sigma^y \rangle = 0$, $\langle \sigma^x\sigma^x \rangle = \langle \sigma^y\sigma^y \rangle$ and translational invariance, the ground state expectation of (3.12) is

$$\begin{aligned} \langle v' \rangle &= \frac{1}{4}(1 + \langle \sigma_1^x(-\tfrac{1}{2}\sigma_3^x) \rangle + \langle \sigma_1^x(-\tfrac{1}{2}\sigma_3^x) \rangle + \langle (\tfrac{\sqrt{3}}{2}\sigma_2^y)(-\tfrac{\sqrt{3}}{2}\sigma_3^y) \rangle \\ &\qquad + \langle (-\tfrac{1}{2}\sigma_2^x)(-\tfrac{1}{2}\sigma_3^y) \rangle) \\ &= \frac{1}{4} - \frac{3}{8}\langle \sigma_o^x\sigma_\delta^x \rangle \quad . \end{aligned} \tag{3.13}$$

To understand why this quantity is non-zero one must consider the number of vortices and antivortices that are present in a lattice tiled with plaquettes of the form in Figure 3.4(a).

But first it is necessary to generate antivortices, which have not yet been obtained on the triangular lattice, the operator v' having only +1 and 0 as eigenvalues. The accomplishment of this task is not difficult. It is in fact not possible to construct a triangular lattice in which all the plaquettes will have axes of quantization as shown in Figure 3.4(a). The plaquettes which form "in-between" these on the bulk lattice will have axes of quantization as shown in Figure 3.4(b), after a rotation of each spin to bring that on site 1 into the orientation shown. For clarification of the geometry involved, see Appendix III, where it is shown that the ground state of the antiferromagnetic plane rotator on the triangular lattice consists of closely packed vortices and antivortices of the form shown in Figure 3.4(a) 1 and (b) 1. From arguments identical to that which lead to (3.12), the antivortex operator v" is found to be

$$v'' = -\frac{1}{4}(1 + \sigma_1^x\sigma_3^v + \sigma_1^x\sigma_2^u + \sigma_2^u\sigma_3^v) \quad . \tag{3.14}$$

Notice that again $v''=(v'')^2$ and $\langle v''\rangle \neq 0$. In fact $\langle v''\rangle=\langle v'\rangle$, so that the interpretation of this operator expectation value is that it gives the (mean) total number of vortices and antivortices in the ground state per plaquette, just as $\langle v^2\rangle$ does on the square lattice. In addition there is an extra factor which arises from the geometry of the triangular lattice. Unlike the situation on the square lattice where there is one square plaquette per lattice site, there are two plaquettes per lattice site on the triangular lattice. The total number

of vortices and antivortices in the ground state per lattice site is then given by

$$\langle v' \rangle = \frac{1}{2} - \frac{3}{4}\langle \sigma_o^x \sigma_\delta^x \rangle \quad , \tag{3.15}$$

and it is this expectation value which will be exhibited as a function of the number of spins per cell, N, in the sequel. This expression involves only the nearest-neighbour spin correlation and so is proportional to the ground state energy per spin.

C. Construction of the Vortex-Antivortex Pair Operators

Now that the vortex operators applicable to the square and triangular lattices have been derived, attention can be focused on other operators that may be interesting, in particular the vortex-antivortex pair operator. The eigenstates of this operator, with non-zero eigenvalue, consist of a vortex configuration about one plaquette and an antivortex about the adjacent plaquette. All other states, including those consisting of adjacent vortices or antivortices, are assigned zero eigenvalue. This operator, or rather the expectation value of this operator, is useful for the estimation of the number of free, unbound vortices in the ground state of the spin ½ XY model.

The pair operator on the triangular lattice will be considered first, since it is simpler to derive than the corresponding operator on the square lattice. The eight configurations which must be considered to derive this

operator are shown in Figure 3.5. The contour over which these configurations are defined is formed by joining two adjacent plaquettes and will be termed a domino both for the triangular and square lattices. Unlike the situation which obtained when the vortex operator was constructed on the triangular lattice, there is no need to consider any other possible domino configurations since all such configurations can be made similar to those shown in Figure 3.5 by transformations in the space group of the lattice and/or a uniform rotation of all the spins. The pair operator p' can then be represented as

$$p' = \frac{1}{8}\,(1 + \sigma_1^x\sigma_2^u + \sigma_2^u\sigma_3^v + \sigma_3^v\sigma_1^x + \sigma_1^x\sigma_4^u + \sigma_2^u\sigma_4^u + \sigma_3^v\sigma_4^u + \sigma_1^x\sigma_2^u\sigma_3^v\sigma_4^u) \quad . \tag{3.16}$$

This formula can be justified by the following argument in which all numbers refer to Figure 3.5, a=x,u,v and i=1,2,3,4. In the configuration 1, all σ_i^a are positive so $\langle p' \rangle$ is 1. When one σ_i^a is negative, as in configurations 2, 3 and 5, the four spin term and three of the two spin terms in p' will be -1, while the three remaining two spin terms are +1 which gives $\langle p' \rangle = 0$. When two of the σ_i^a are negative, as in configurations 4, 6 and 7, four of the six spin terms (those containing at least one of the negative σ_i^a) will be -1, while the other terms in p' will be +1 so that $\langle p' \rangle$ is again zero. Finally when three of the σ_i^a are negative, as in configuration 8, the four spin term is negative as is each of the three two spin terms containing the one remaining positive σ_i^a ; all other terms will

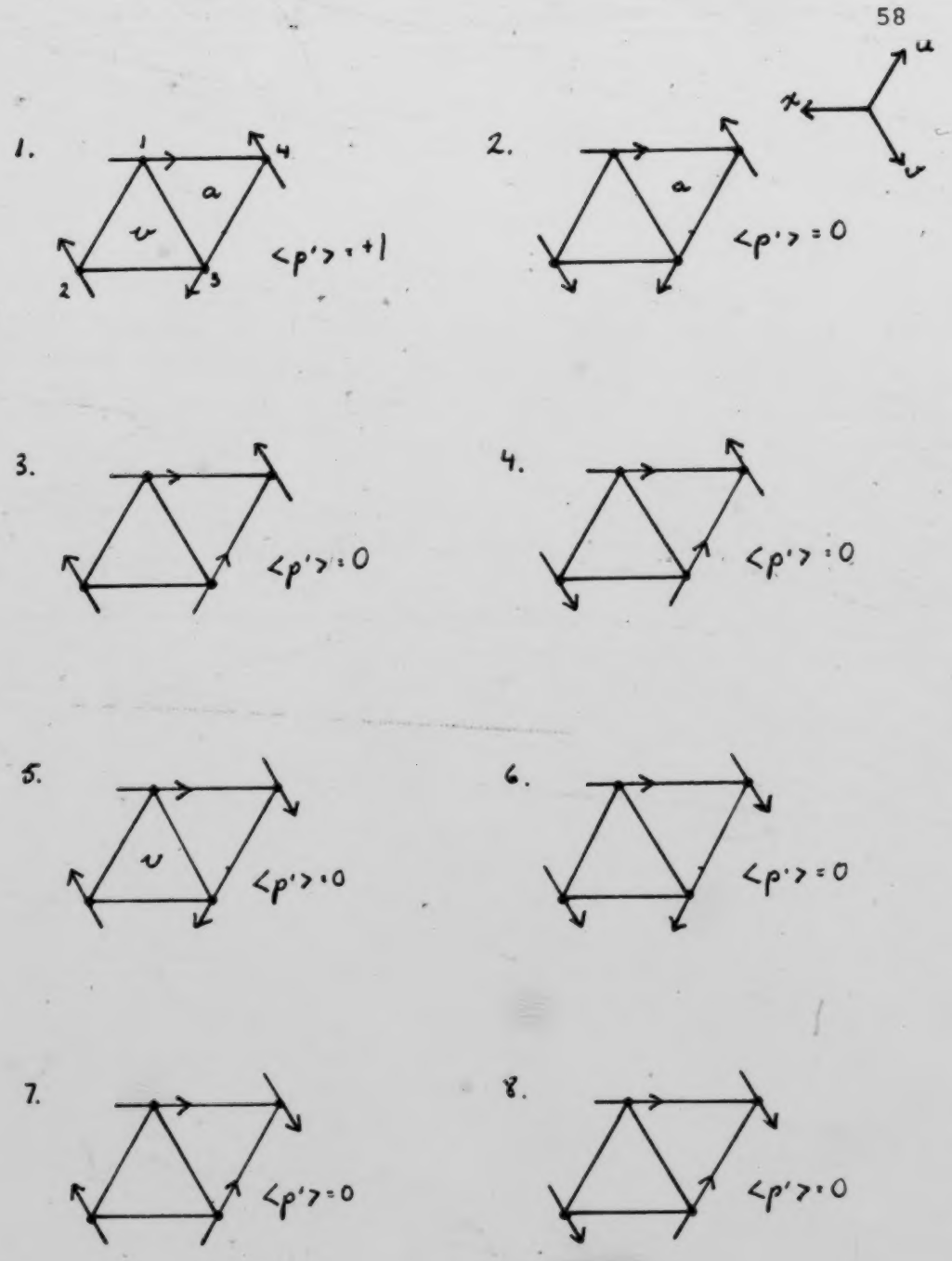

Figure 3.5 - Vortex-antivortex pair states on the triangular lattice. (v≡vortex, a≡antivortex)

again be +1 so that $\langle p' \rangle = 0$ in this case as well. It is also straightforward to observe that $p' = (p')^2$. The implication of this result for the interpretation of the expectation value of p is that p does not discriminate between a pair which is a v(ortex)-a(ntivortex) and one which is a.-v. This result is in fact obvious from the derivation of p'. In calculating $\langle p' \rangle$, use is made of the following relations:

$$\langle \sigma_1^x \sigma_2^u + \sigma_2^u \sigma_3^v + \sigma_3^v \sigma_1^x \rangle = -\frac{3}{2} \langle \sigma_o^x \sigma_\delta^x \rangle \quad , \tag{3.17}$$

$$\langle \sigma_1^x \sigma_4^u \rangle = \langle \sigma_3^v \sigma_4^u \rangle = -\frac{1}{2} \langle \sigma_o^x \sigma_\delta^x \rangle \quad , \tag{3.18}$$

$$\langle \sigma_2^u \sigma_4^u \rangle = \langle \sigma_o^x \sigma_{\sqrt{3}\delta}^x \rangle \quad . \tag{3.19}$$

In addition, the expectation value $\langle \sigma_1^x \sigma_2^u \sigma_3^v \sigma_4^u \rangle$ can be simplified before evaluation by rotating the axes u, v, x by 120^o according to x→v, v→u and u→x. The ground state expectation value is invariant under this transformation since H_{XY} is invariant under this, and any, rotation in the x-y, or x-u-v, plane; the desired four spin correlation becomes

$$\langle \sigma_1^v \sigma_2^x \sigma_3^u \sigma_4^x \rangle = \frac{1}{4} \langle \sigma_1^x \sigma_2^x \sigma_3^x \sigma_4^x \rangle - \frac{3}{4} \langle \sigma_2^x \sigma_4^x \sigma_1^y \sigma_3^y \rangle \quad . \tag{3.20}$$

Using the results (3.17)-(3.20), the expectation value of p' can be written as

$$\langle p' \rangle = \frac{1}{8} - \frac{5}{16} \langle \sigma_o^x \sigma_\delta^x \rangle + \frac{1}{8} \langle \sigma_o^x \sigma_{\sqrt{3}\delta}^x \rangle + \frac{1}{32} \langle \sigma_1^x \sigma_2^x \sigma_3^x \sigma_4^x \rangle - \frac{3}{32} \langle \sigma_2^x \sigma_4^x \sigma_1^y \sigma_3^y \rangle . \tag{3.21}$$

This result measures the (mean) number of vortex-antivortex pairs per domino , in the ground state of the spin ½ XY model on the triangular lattice. On this lattice however, there are three different domino patterns per lattice site so that the expectation value which will be reported in the next section, giving the number of vortex-antivortex pairs per lattice site , is

$$\langle p' \rangle = \frac{3}{8} - \frac{15}{16}\langle \sigma_o^x \sigma_\delta^x \rangle + \frac{3}{8}\langle \sigma_o^x \sigma_{\sqrt{3}\delta}^x \rangle + \frac{3}{32}\langle \sigma_1^x \sigma_2^x \sigma_3^x \sigma_4^x \rangle - \frac{9}{32}\langle \sigma_2^x \sigma_4^x \sigma_1^y \sigma_3^y \rangle \quad . \tag{3.22}$$

The pair operator p which is applicable to the square lattice can of course be derived from similar considerations. In this case however the domino made up of two adjacent square plaquettes contains six lattice sites and even though the spin on one site may be fixed there are still 32 pair states which must be considered in the derivation of p. Several of these are shown in Figure 3.6. It is actually an easier task to derive p^2 directly rather than construct p and square the resulting operator. At any rate the procedure is straightforward, if somewhat tedious and the final result can be written down without consideration of the details of derivation as

$$\begin{aligned} 16p^2 = 1 &+ \sigma_1^x\sigma_5^x + \sigma_4^y\sigma_6^y - \sigma_1^x\sigma_3^x - \sigma_3^x\sigma_5^x - \sigma_2^y\sigma_4^y - \sigma_2^y\sigma_6^y + \sigma_1^x\sigma_4^x\sigma_5^y\sigma_6^y \\ &+ \sigma_1^x\sigma_3^x\sigma_2^y\sigma_4^y + \sigma_5^x\sigma_3^x\sigma_2^y\sigma_6^y + \sigma_1^x\sigma_3^x\sigma_2^y\sigma_6^y + \sigma_5^x\sigma_3^x\sigma_2^y\sigma_4^y - \sigma_1^x\sigma_3^x\sigma_4^y\sigma_6^y \\ &- \sigma_5^x\sigma_3^x\sigma_4^y\sigma_6^y - \sigma_1^x\sigma_5^x\sigma_2^y\sigma_4^y - \sigma_1^x\sigma_5^x\sigma_2^y\sigma_6^y \quad , \end{aligned} \tag{3.23}$$

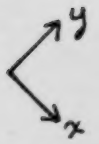

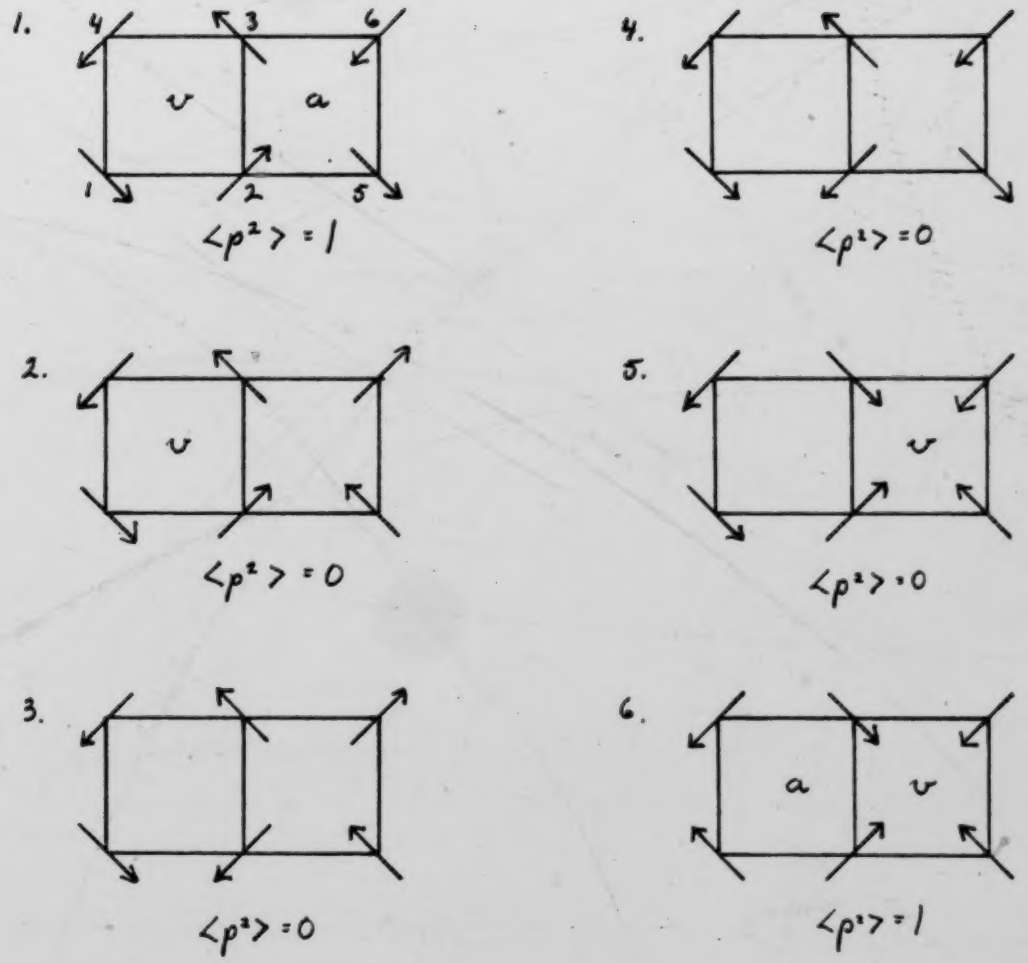

Figure 3.6 - Selected vortex-antivortex pair states on the square lattice. (v≡vortex, a≡antivortex)

where the numbering is given in Figure 3.6. In taking the expectation value of (3.23) notice must be taken of the number of dominoes per lattice site, on an N site cell, which on the square lattice is just two. Including this correction factor leads to the expectation value

$$\langle p^2 \rangle = \frac{2}{16} \left(1 + 2\langle \sigma_o^x \sigma_{2\delta}^x \rangle - 4\langle \sigma_o^x \sigma_{\sqrt{2}\delta}^x \rangle + \langle \sigma_1^x \sigma_5^x \sigma_4^y \sigma_6^y \rangle + 2\langle \sigma_1^x \sigma_3^x \sigma_2^y \sigma_4^y \rangle + 2\langle \sigma_1^x \sigma_3^x \sigma_2^y \sigma_6^y \rangle - 4\langle \sigma_1^x \sigma_3^x \sigma_4^y \sigma_6^y \rangle\right) \qquad (3.24)$$

which represents the (mean) number of vortex-antivortex pairs, per lattice site, in the ground state of the spin ½ XY model on the square lattice.

D. Presentation and Discussion of Results

It is a simple matter now to match the expressions for $\langle v^2 \rangle$, $\langle v' \rangle$, $\langle p' \rangle$ and $\langle p^2 \rangle$ given above and the various two and four spin correlations presented in Chapter 2, section E, to determine the vorticity and pair vorticity operators as functions of 1/N. These are presented in Table 3.1 and, graphically, in Figures 3.7 and 3.8. Notice that considerations of time and expense have limited the calculation of $\langle p' \rangle$ to the 9 and 13 spin cells. This quantity is not presented for the 7 spin cell because this particular cell does not allow the calculation of second-nearest neighbour correlations, every site being a nearest neighbour to each other site.

Both $\langle v' \rangle$ and $\langle v^2 \rangle$ are seen to behave in an approximately linear fashion as functions of 1/N, although there is a

Table 3.1 - Vorticity and pair vorticity for the spin ½ XY model on the (a) square and (b) triangular lattices.

(a)

N	8	10	16	18
$\langle v^2 \rangle$	0.01134	0.01432	0.01861	0.01926
$\langle p^2 \rangle \times 10^3$	5.68	3.79	9.46	9.62
v_{free}	~ 0	3.37×10^{-3}	~ 0	~ 0

(b)

N	7	9	13	19
$\langle v' \rangle$	0.07144	0.07922	0.08710	0.09206
$\langle p' \rangle$	-	0.05244	0.05718	-
v_{free}	-	-0.01283	-0.01363	-
$[v^*_{free}$	-	0.00691	0.00774	-]

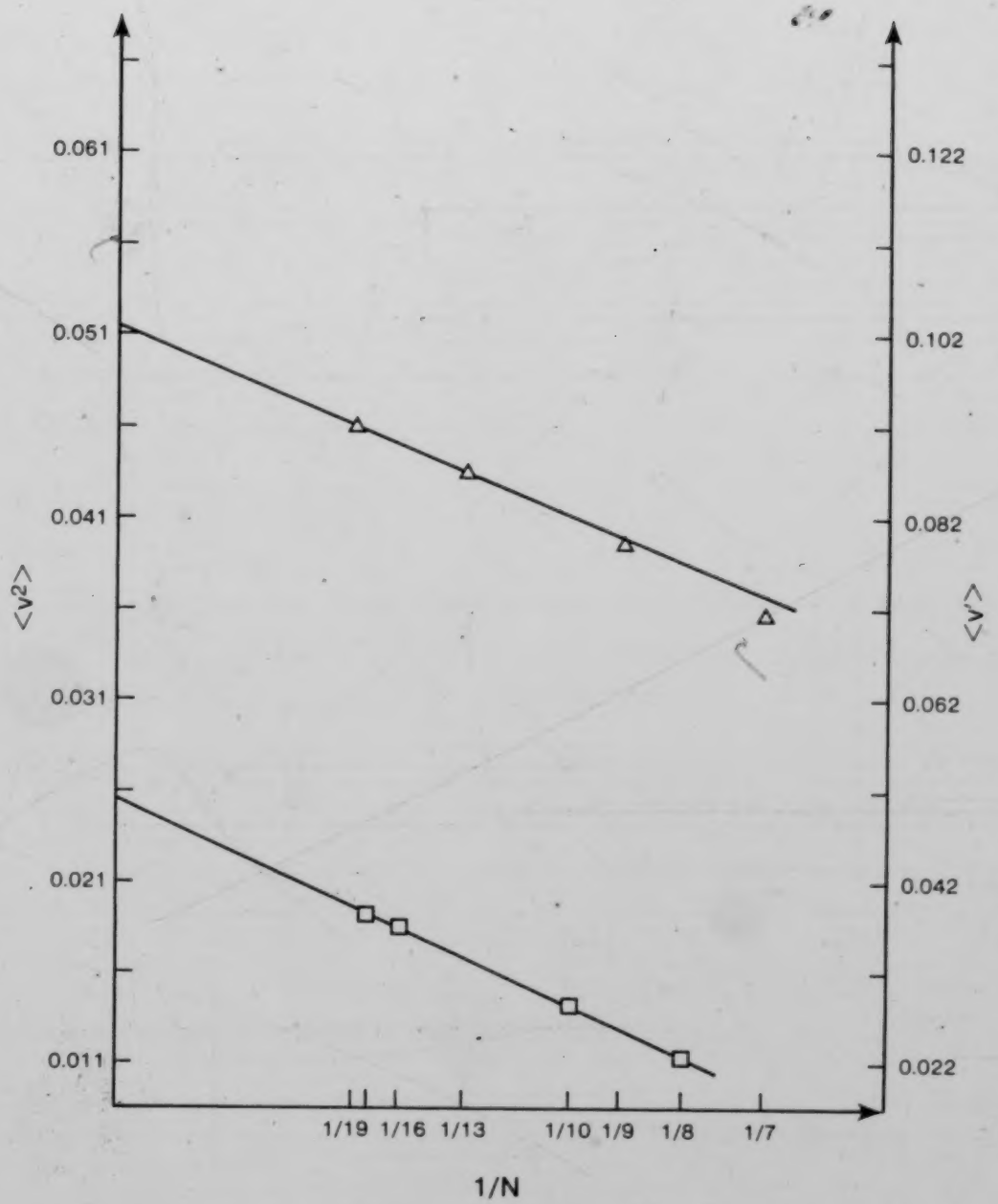

Figure 3.7 - Expectation values of vortex operators for the square (squares, left-hand scale) and triangular (triangles, right-hand scale) as functions of 1/N.

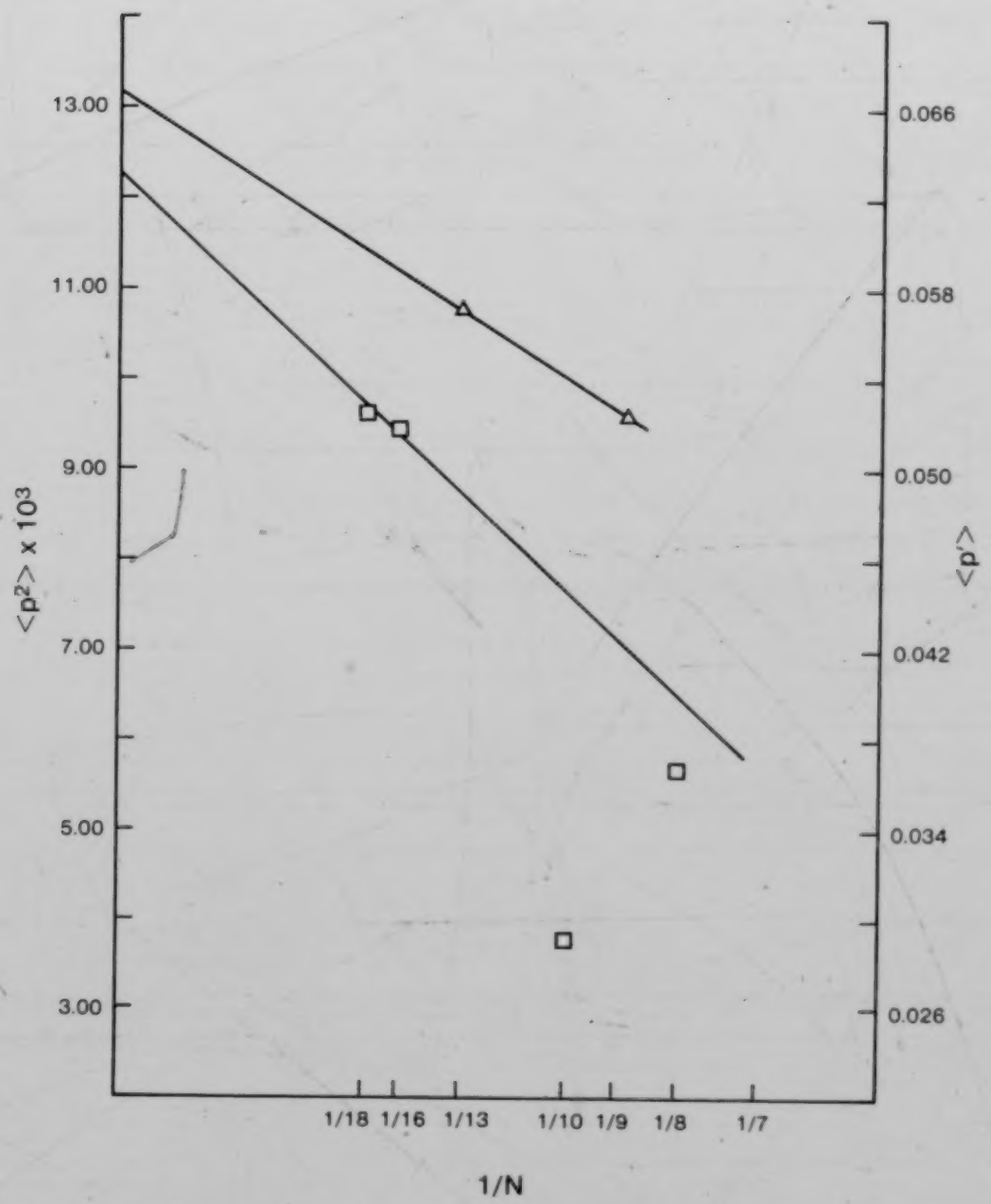

Figure 3.8 - Expectation values of vortex-antivortex pair operators for the square (squares, left-hand scale) and triangular (triangles, right-hand scale) lattices as functions of 1/N.

distinct curvature to the results, especially noticeable for $\langle v' \rangle$. Because of this the best fit line used to extrapolate these quantities was drawn with a bias in favor of the larger N data and the estimated uncertainty in these extrapolations raised accordingly. For $\langle v^2 \rangle$ the value found for the infinite square lattice is 0.025±0.002, while the value of $\langle v' \rangle$ for the infinite triangular lattice is found to be 0.104±0.008. It seems at this point to be coincidental that the latter number is slightly more than four times the former extrapolation. The situation with regard to $\langle p^2 \rangle$ and $\langle p' \rangle$ is less certain. Only two data points are available from which to determine a value of $\langle p' \rangle$ in the infinite lattice limit. The value obtained for this quantity, 0.067±0.010, has a correspondingly larger uncertainty. The data varies widely but an extrapolation of $\langle p^2 \rangle_N$ to the infinite lattice case of $(1.23\pm0.10)\times10^{-2}$ can be quoted, with very limited accuracy. With regard to this curve however it is interesting to note that if $\langle p^2 \rangle_{10}$ were doubled, the improvement in the data would be such as to allow an extrapolation to be made with some confidence, although the same negative curvature of the data as observed in the vorticity operators would be present. Needless to say the calculations leading to $\langle p^2 \rangle_{10}$ have been checked many times for accuracy. If some error is present, it is likely due to a geometric factor, a result of the fact that of the four even N cells on the square lattice, only the N=10 cell was not reflection invariant and so has a smaller symmetry group than the others. More will be said on this subsequently.

The interpretation of the results presented above begins with examination of the infinite temperature limit of the operator expectation values $\langle v^2 \rangle$, $\langle v' \rangle$, $\langle p^2 \rangle$ and $\langle p' \rangle$. In this limit all correlations are zero and the components of the site spin operators are distributed randomly. The vorticity per lattice site on the square lattice is then 0.250. This in turn means that the number of vortices per lattice site, or equivalently, per plaquette is 0.125, which is not in agreement with the infinite temperature limit obtained in section A for the classical ($s=\infty$) XY model. The expectation value of v', in this limit, is 0.500, which has an interpretation as the average number of vortices and antivortices, per lattice site, on the triangular lattice. Recalling that on this lattice there are 2 plaquettes per site and that the number of vortices is equal, by symmetry, to the number of antivortices, this result predicts that the number of vortices per plaquette, on the triangular lattice, in the infinite temperature limit, to be 0.125. Notice that this number is in agreement with the similar result derived for the classical XY model on this lattice in section A. The values assumed by $\langle p^2 \rangle$ and $\langle p' \rangle$ in the infinite temperature limit are 0.125 and 0.375 respectively. Although the corresponding limits in the $s=\infty$ XY model have not been calculated, it would be straightforward to do so. What can be said in this regard is that the number of vortex-antivortex pairs found in the infinite temperature limit, on both lattices, is greater than that expected by assuming the probability of finding a pair is just

the product of the probability of locating a vortex and that of locating an antivortex. It seems that, even in the infinite temperature limit, the chance of finding an antivortex (or a vortex for that matter) adjacent to a vortex is enhanced relative to that of finding one of these structures alone. This is actually reasonable when it is noted that, on the triangular lattice for example, a vortex configuration on a plaquette involves the orientation of spins at three lattice sites while the addition of an antivortex to the adjacent plaquette is dependent only on the orientation of the spin on the one remaining site which defines the domino . A similar situation occurs on the square lattice.

In the ground state of the classical ($s=\infty$) XY model, which consists of all spins aligned in some arbitrary direction in the x-y plane, there are no vortices. This is consistent with the view that the vortices, and antivortices, are topological excitations whose numbers grow as a function of T. In contrast with this is the result derived above, that the number of vortices and antivortices per lattice site in the ground state of the spin ½ XY model is 0.025 ± 0.002 on the square lattice and 0.104 ± 0.008 on the triangular lattice. This is to be considered along with the fact that the ground state of this model shows partial long-range order, in the form of a non-zero transverse magnetization per site. This order is not total, leaving enough local disorder to allow the presence of vortices and antivortices, for it is the nature of these excitations to arise as local magnetic order gives way to

disorder. The origin of both this disorder and the non-zero vorticity at zero temperature is of course quantum mechanical, with the Hamiltonian H_{XY} composed of the non-commuting operators S_i^x, S_i^y, so that the ground state cannot be an eigenstate of either operator. It is interesting to note that while the transverse magnetizations on the square and triangular lattices differ by only ~4% (see Marland and Betts, [1.17]) the vorticity per lattice site on the triangular lattice is almost exactly four times that found for the square lattice. This is only part of the evidence which indicates that understanding of the combinatorics of vorticity on different lattices is far from complete.

Once the vorticity, $\langle v^2 \rangle$ and $\langle v' \rangle$ and the pair vorticity, $\langle p^2 \rangle$ and $\langle p' \rangle$, are known it is interesting to try to calculate the number of free vortices present in the ground state of the spin ½ XY model. By "free vortices" what is meant are all those vortices (or anti-vortices) which are not members of a vortex-antivortex pair or some other larger cluster. With only the total vorticity and the number of vortex-antivortex pairs, from $\langle p^2 \rangle$ and $\langle p' \rangle$, available, it is clear that the effect of larger clusters must be ignored in the calculation of the number of free vortices. For the square lattice, where the density of vortices and antivortices is ~2.5% this contribution is likely negligible. For the triangular lattice this density is ~10% and the effect of clusters becomes more important. This should be kept in mind when interpreting the results presented below.

The number of free vortices per site is obtained by associating one bound vortex with every pair and subtracting the number of bound vortices from the total number of vortices. The latter number is of course given by half the total number of vortices and antivortices , obtained from $\langle v^2 \rangle$ and $\langle v' \rangle$. In terms of operator expectation values the number of free vortices per site on the square lattice is then

$$v_{free} = \frac{1}{2}\langle v^2 \rangle - \langle p^2 \rangle \quad , \tag{3.25}$$

and on the triangular lattice is

$$v_{free} = \frac{1}{2}\langle v' \rangle - \langle p' \rangle \quad . \tag{3.26}$$

The values obtained for this quantity are shown in Table 3.1. The results on the square lattice are, with one exception, all consistent with zero in the sense that $v_{free} < 10^{-4}$ which is of the same order as the uncertainty in $\langle v^2 \rangle_N$ and $\langle p^2 \rangle_N$ introduced by the numerical computations. The exception occurs for N=10 and although v_{free} is still small in absolute magnitude it is of the same order as $\langle p^2 \rangle_{10}$. In fact, if as mentioned above, the value of $\langle p^2 \rangle_{10}$ were doubled, then the number of free vortices per site for this cell would, with a slight extension of the uncertainty limit to $\sim 2\times10^{-4}$, also be consistent with zero. The results for the triangular lattice do not conform as well with expectation. The number of free vortices per site is both relatively large, 30% of $\langle v' \rangle/2$, and negative! It should be noted however that in absolute terms

free vortices are predicted to occupy only ∿-1% of the lattice sites. Possible interpretations of and explanations for this finding will be speculated upon in the following chapter.

Finally, it is interesting to compute the number of free vortices per site for the infinite lattice, on the basis of the extrapolations made from Figures 3.7 and 3.8. For the square lattice, the calculation yields $v_{free}=2\times10^{-4}$ which, in view of the large uncertainty of 0.001 in $\langle p^2\rangle_\infty$, is consistent with zero. The result obtained for the triangular lattice is $v_{free}=-0.097\pm0.038$ which is not consistent with zero free vortices per site, even with the inclusion of a large uncertainty in $\langle p'\rangle_\infty$, and which is in fact not physically possible.

[After the completion of the main body of this work, a new formula for the number of free vortices in the ground state of the spin ½ XY model on the triangular lattice was obtained {4.2}. Let p(v) be the probability of finding a vortex on any given plaquette of the triangular lattice and p(v;0) the conditional probability that an adjacent plaquette contains neither a vortex nor an antivortex. Since each plaquette on the triangular lattice has three adjacent neighbours, the probability of finding an isolated (or free) vortex is just

$$p(v)\cdot(p(v;0))^3 \quad .$$

This then also represents the number of free vortices present per lattice site. On the triangular lattice $p(v)=\langle v'\rangle/2$.

The probability p(v;0) is equal to 1-p(v;a) where p(v;a) is the conditional probability that a plaquette adjacent to one on which a vortex is situated is itself occupied by an anti-vortex (or vortex). Neglecting correlations between next-nearest neighbour plaquettes (third neighbour and higher order site correlations), p(v;a) is just the probability of finding a vortex-antivortex pair per domino, $\langle p' \rangle/3$, divided by the probability that the adjacent site is occupied by an antivortex, $\langle v' \rangle/2$. The new relation which gives the approximate number of free vortices is then

$$v^*_{free} = \frac{\langle v' \rangle}{2} \left(1 - \frac{2\langle p' \rangle}{3\langle v' \rangle}\right)^3 \quad . \tag{3.27}$$

Expanding this formula to first order in $\langle p' \rangle/\langle v' \rangle$ gives equation (3.26). This new relation is an improvement over the old in that it gives a direct measure of the number of free vortices, although it still neglects the effects of clusters of three or more vortices/antivortices in the expression for p(v;a).

Using the values of $\langle v' \rangle$ and $\langle p' \rangle$ in Table 3.1b), it is found that for the 9-spin cell $v^*_{free}=0.00691$ while for the 13-spin cell $v^*_{free}=0.00774$. An obvious improvement over the previous values for the number of free vortices is that v^*_{free} is positive for both values of N for which data is available. These numbers are also smaller in absolute value than the previous estimates, being $\sim$10% of the respective $\langle v' \rangle$, although they are still not small enough to be consistent with $v^*_{free} \simeq 0$.

What is yet to be calculated is the expectation value of the free vortex operator which is introduced in Chapter IV, section B. It is expected that such a quantity, to which (3.27) is only an approximation, would be consistent with an absence of free vortices in the spin ½ XY model ground state.]

CHAPTER IV

SUMMARY AND DISCUSSION

A. Ground State Energy and Correlations

The main numerical result of Chapter II was that the ground state energy of the spin ½ XY model, on the square lattice, as extrapolated to the infinite lattice case through the results of calculations on cells with an even number of spins was not shown to be equal to that obtained from similar calculations on a series of cells containing an odd number of spins. The corresponding energies are $E_o^{(even)}/NJ = -1.078 \pm 0.002$ and $E_o^{(odd)}/NJ = -1.07 \pm 0.01$. The uncertainties quoted here are due mainly to the extrapolation procedure, with computing errors accounting for, at most, 5.0×10^{-4}. Certainly before any conclusion can be reached, the ground state energy for N=17, which is the last odd number of sites per cell for which calculations are now feasible, must be obtained. The results of the even N calculations indicate that the N=17 data point should not lie more than ±0.004 units from the line already obtained from the two odd N data points. Such a deviation is more than enough however to bring the two extrapolated ground state energies into agreement. Although such a course may be premature it is interesting to speculate on any disagreement between the infinite lattice energies $E_o^{(even)}/NJ$ and $E_o^{(odd)}/NJ$ remaining after the N=17 result has been calculated.

The source of any discrepancy may be due to the fact that the periodic boundary conditions force a tiling of the

infinite square lattice with domains of $m_z=\frac{1}{2}$. If just two such cells of dimension, e.g., 9 are considered, the result is a configuration of 18 spins with a total m_z of 1, which is taken to contribute to the ground state of the infinite lattice. The argument of Mattis, as presented in Chapter II, would imply that for this 18 spin block the ground state has $m_z=0$. An extra "domain wall" energy has been added that does not disappear in the infinite lattice limit, thus raising the ground state energy calculated from cells with an odd number of spins relative to that obtained from even N cells. If this is the case, better agreement may be found by taking "anti-periodic" boundary conditions for odd N cells, in which spins on sites in the cell boundary are linked, not to other spins on boundary sites, but to the opposite spins on the same boundary sites. Such a procedure would change the symmetry properties of the cell, but it would have the effect of patching together cells with opposite net m_z, to build up an infinite lattice which at each stage has the correct m_z, according to Mattis' arguments, of the ground state.

The lack of a reliable extrapolation for the two spin correlations on the square lattice presented in Chapter II has already been mentioned. To eliminate the degeneracy of the second and third-nearest neighbour correlations for cells with $N\leq 16$ which seems to be creating the difficulties, one might believe that performing calculations on cells with less symmetry than the square cells considered here would be effective. Such calculations were however carried out early

in the development of the finite cell method. The results showed no pattern at all. This would seem to indicate that a family of cells which share the same symmetry properties is an important factor in achieving linearity with this method. The four spin correlations presented in Chapter II are even more erratic as functions of N and no reliable extrapolations can be obtained for these. The problem here seems to be related to cell size and until such time as calculations with cells of N>18 are feasible other avenues must be explored. Once the question of the ground state energy for cells with an odd number of spins is settled, correlations may be calculated for these cells. The extra data points, while not as useful as results for N>18, would likely give an indication as to the direction in which extrapolation is most reliable. As for the correlations on the triangular lattice the above remarks may certainly apply, but the immediate concern is to generate the four spin correlations for N=19 and see whether or not the results form a straight line, before apologizing for the lack of linearity and a reliable extrapolation.

To close this section a comment on the applicability of the method described in Chapter II to other models besides those already considered {1.15}-{1.17} is in order. An example of such a model is the Ising model in a transverse field, described by the Hamiltonian:

$$H = -J \sum_{<i,j>} S_i^z S_j^z - \Gamma \sum_i S_i^x \quad . \tag{4.1}$$

This model is particularily interesting since Suzuki has proven {4.1} the equivalence of the ground state of (4.1) with that of the three-dimensional Ising model, at all finite temperatures. Unfortunately, this model is not amenable to analysis by the finite cell method since there appears to be no simple many-body operator such as $M_Z = \sum_i S_i^z$, which commutes with H and thus provides a good quantum number to label the energy states, in particular the ground state. The entire space of states, of dimension 2^N for a cell of N spin ½'s, would seem to contribute to the ground state and for N≥10, even taking the symmetry of the cell into account, computations are at present unfeasible. The XY model in a longitudinal field does not suffer from this defect, since M_Z still commutes with the Hamiltonian.

$$H = -2J \sum_{<i,j>} (S_i^x S_j^x + S_i^y S_j^y) - \Gamma \sum_i S_i^z \quad , \qquad (4.2)$$

and although m_z is not necessarily zero in the ground state for a certain range of the parameter Γ/J, the calculations involved are no more complex than those already carried out for H_{XY}. Such calculations remain to be performed.

B. Vortices and Free Vortices

The results of the calculation of the total number of vortices and antivortices per lattice site in the ground state of the spin ½ XY model are $\langle v^2 \rangle_\infty = 0.025 \pm 0.002$ on the square lattice and $\langle v' \rangle_\infty = 0.104 \pm 0.008$ on the triangular lattice. This is unlike the situation in the ground state

of the classical (s=∞) XY model, which contains no vortices or antivortices. The interpretation of these findings in terms of partial long-range order and local disorder has already been made in the previous chapter. A comment also made previously but which bears repeating deals with the relative magnitudes of the total vorticity on the square and triangular lattices. Although it is certainly not a definite indication of any relation, the fact that the triangular lattice result is almost exactly four times the square lattice result suggests a geometric interpretation may be possible for this difference, especially in view of the fact that the transverse magnetization, which signals long-range order, is so similar on both lattices. Another integer factor arises when the expectation value of the pair operator for the N=10 cell on the square lattice is considered. The individual two and four spin correlations which contribute to $\langle p^2 \rangle_{10}$ do not seem to lie outside of the expected range, but an examination of Figure 3.8 as well as consideration of the free vortices per site for the N=10 cell indicates that a value of $\langle p^2 \rangle_{10}$ twice that obtained would be in better agreement with the other results on the square lattice. The only place for such a factor to enter is through the geometry of the cell. There is a clue here as well, for the N=10 cell is the only one considered on the square lattice which was not reflection invariant. The exact effect this might have on the calculation of $\langle p^2 \rangle_{10}$ is unknown, but it does suggest that cell geometry plays a larger role than assigned in the determination of

vorticity and pair vorticity.

In the classical ($s=\infty$) XY model, in two dimensions of course, the introduction of vortices and antivortices as excitations of the system has allowed an intuitive picture of the phase transition which has been predicted for this model to be developed. Vortex-antivortex pairs are created as temperature rises, until, at the critical temperature, these pairs unbind (the vortex-antivortex "dipoles" are "ionized") and the long range order which characterizes the low temperature phase is lost. A phase transition has also been predicted in the spin ½ XY model and so an interesting quantity to calculate in the ground state of this model is the number of free vortices, those which are not found adjacent to an antivortex. Although the number of vortices in the ground state of the spin ½ XY model is non-zero, the number of free vortices is expected to be zero.

Results of the calculation of the number of free vortices in the ground state of the spin ½ XY model on the square lattice confirm, with the one well-noted exception discussed above, the predicted value of zero. This result holds in the infinite lattice limit as well. The number of free vortices on the triangular lattice, as derived above, is not consistent with zero and is in fact negative, a result which holds in the infinite lattice limit as well. The origin of this result seems to be the larger density of vortices and antivortices which occurs in the ground state on the triangu-

lar lattice relative to the square lattice. The numbers are 10.4% relative to 2.5%. When this density increases, the number of pairs which are free decreases as larger clusters of three and four vortices/antivortices are formed. When this occurs it is no longer true that one vortex is associated with every vortex-antivortex pair as for example a cluster of two vortices and two antivortices on the triangular lattice will contain 3 such pairs. The number of bound vortices will be overestimated and the number of free vortices obtained from the relation (3.23) may even be negative. As an example consider the anti-ferromagnetic ground state of the classical ($s=\infty$) XY model on the triangular lattice (see Appendix III). In this case the number of pairs per domino is 1, since the state is "packed" with vortices and antivortices and every domino contains a pair. The number of pairs per site is 3. The number of vortices per plaquette is $\frac{1}{2}$, every site being occupied by either a vortex or antivortex, which occur in equal numbers, so that the number of vortices per site is 1. Using (3.23) to calculate the number of free vortices, one finds this number to be -2! The reason for this should now be apparent. Just as there really are no free vortices in this state, there are no free pairs either. Every pair is in turn a member of some higher order cluster which in turn is part of an even larger cluster, and so on ad infinitum. There are no sites in the lattice for this state which are not occupied by a vortex or antivortex. The simple formula (3.23) is not applicable then in situations where the total number of

pairs and the total number of free pairs are not the same.

It would then seem reasonable to conjecture that the fact that equation (3.23) predicts a negative number of free vortices on the triangular lattice is an indication that the number of three and especially four-member clusters of vortices and antivortices is non-zero in the ground state of the spin ½ XY model on the triangular lattice. This result also suggests that the number of free vortices is indeed zero in the ground state on this lattice.

Verification of this can be sought in the calculation of the expectation value of the free vortex operator which has recently been calculated {4.2} for the triangular lattice. The eigenstates of this operator are taken to be those in which a vortex situated on a central plaquette is surrounded on the three adjacent plaquettes by configurations exhibiting no vorticity. A total of six sites are involved and the expectation value of this operator involves all three two spin correlations (first, second and third-nearest neighbour), all inequivalent four spin correlations and several six spin correlations . Pressures of time have not allowed the evaluation of this operator, although it is straightforward to accomplish. It should be noted however that because correlations between spins up to third-nearest neighbour in distance must be evaluated, calculations would be required on the 19-spin cell in order to achieve an accurate extrapolation to the infinite lattice. Since in fact the 9 and 13-spin cells do not have third nearest neighbours, a simpler free vortex

operator can be derived which is applicable to these cells. In principle the same operator could be determined for the square lattice. A number of reasons suggest this would be of little use. First, the number of free vortices in the ground state of the spin ½ XY model on the square lattice has been estimated to be zero using the approximate relation (3.22). Secondly the construction of such an operator would involve consideration of configurations over twelve sites and although possible, it would be likely that computer assistance would be necessary to complete the derivation. Finally, such an operator would involve correlations between spins separated by a distance of up to $\sqrt{10}\,\delta$, and it is likely that the numerical results for the 16 and 18 spin cells, the only two for which this operator expectation value exists, would not be enough to allow for an accurate extrapolation to the infinite lattice.

C. Experiments on Two-Dimensional Systems

The discussions to this point have all been of a theoretical character, with little mention of experiment. The Kosterlitz-Thouless theory has been taken as the description of the phase transition in the planar model and competing theories have been neglected. The reason this approach can be taken is that experimental evidence now favors the Kosterlitz-Thouless picture over those of other investigators. To discuss these experiments however, one final theoretical result is needed. Applying the Kosterlitz-

Thouless theory to neutral superfluids, Nelson and Kosterlitz {4.3} discovered a simple relationship between superfluid density, ρ_s, and the critical index $\eta(T)$.

$$\frac{\rho_s(T)}{T} = \frac{2\pi m^2 k_B}{h^2 \eta(T)} \quad , \tag{4.3}$$

where m is the mass of a Helium atom, h is Planck's constant and the index $\eta(T)$ is defined from the spin-spin correlation function by

$$\Gamma(\vec{r}) = \langle S_o^x S_{\vec{r}}^x \rangle = r^{-\eta(T)} \tag{4.4}$$

for $T<T_c$. The relation (4.3) holds in the limit as $T \to T_c$ from below. Thus a measurement of the jump in the superfluid density ρ_s at the critical temperature can be compared with the value predicted from (4.3) for this quantity:

$$\lim_{T \to T_c^-} \{\frac{\rho_s(T)}{T}\} = \frac{2\pi m^2 k_B}{h^2 \eta(T_c)} \quad . \tag{4.5}$$

The Kosterlitz-Thouless theory {1.14}, {4.4} predicts the universal result $\eta(T_c)=\frac{1}{4}$ which leads from (4.5) to

$$\lim_{T \to T_c^-} \{\frac{\rho_s(T)}{T}\} = 3.491 \times 10^{-9} \ g/cm^2\text{-}K \quad .$$

Several experiments have now been carried out which measure the superfluid density at the transition. Rudnick and collaborators, beginning in 1969, had performed measurements of third sound propagation in thin He^4 films {4.5} and a reanalysis of this earlier data yields {4.6}

$$\frac{\rho_s(T_c)}{T_c} = (3.30 \pm 0.21)\times 10^{-9}\ g/cm^2\text{-}K \quad .$$

Bishop and Reppy {4.7} have measured the superfluid transition in two-dimensional He^4 films by "shaking" the fluid, using the Andronikashvili torsional-oscillator technique. A helium film is adsorbed on a Mylar film substrate. A strip is wound up into a cylinder and oscillated at the resonant frequency. When a helium film of the desired thickness, usually one or two monolayers, has been deposited, measurements of the period and Q factor of the oscillator are made to determine the temperature dependence of the superfluid mass and dissipation. The value obtained for $\rho_s(T_c)/T_c$ is

$$(3.5 \pm 0.5)\times 10^{-9}\ g/cm^2\text{-}K \quad .$$

These experiments give strong support to the Kosterlitz-Thouless version of the planar critical behaviour and also appear to eliminate several competing theories which predict other values for $\eta(T_c)$.

Other systems of experimental interest include {4.8}, the solid formed by electrons on the surface of liquid helium, at sufficiently low temperatures and high electron density, various systems liquid crystals, lipid layers floating on a water surface and layers adsorbed on a crystalline substrate. All of these systems can be discussed in terms of the theory

of two-dimensional melting {1.11}, with various modifications, but at the moment no firm connection between theory and experiment has been made. In fact the electron solid has only recently been observed {4.9}, using a radio-frequency resonance technique. Another recent discovery is the construction of an physical system which is apparently a two-dimensional spin ½ XY antiferromagnet. The system consists of crystals of $(Co(p\text{-methyl-pyridine N-oxide})_6)(ClO_4)_2$ {4.10}, with the Co^{+2} ion in a high ligand field possessing spin ½. At finite ($T \sim T_c$ and above) temperatures, the spin ½ XY model is also applicable to a variety of magnetic insulators {4.11}, although experimental systems which remain well described by the XY model at very low ($T \ll T_c$) temperatures have not yet been discovered. It remains very much an experimental challenge to provide results which will complement theoretical findings on the nature of the phase transition in the two-dimensional spin ½ XY model.

BIBLIOGRAPHY

{1.1} R.E. Peierls, Ann. Inst. Henri Poincare 5 (1939).

{1.2} N.D. Mermin, Phys. Rev. 176 (1968) 250.

{1.3} N.D. Mermin and H. Wagner, Phys. Rev. Lett. 22 (1966) 1133.

{1.4} P.C. Hohenberg, Phys. Rev. 158 (1967) 383.

{1.5} B.J. Alder and T.A. Wainwright, Phys. Rev. 127 (1962) 359.

{1.6} H.E. Stanley and T.A. Kaplan, Phys. Rev. Lett. 17 (1966) 913.

{1.7} H.E. Stanley, Phys. Rev. Lett. 20 (1968) 589;
M.A. Moore, Phys. Rev. Lett. 23 (1969) 861;
K. Yamaji and J. Kondo, J. Phys. Soc. Japan 35 (1973) 25.

{1.8} D.D. Betts, C.J. Elliott and R.V. Ditzian, Can. J. Phys. 49 (1971) 1327;
J. Rogiers, E.W. Grundke and D.D. Betts, Can. J. Phys. 57 (1979) in the press.

{1.9} J.M. Kosterlitz and D.V. Thouless, J. Phys. C5 (1972) L24; J. Phys. C6 (1973) 1181.

{1.10} F.R.N. Nabarro, Theory of Crystal Dislocations (Pergamon Press, Oxford, 1967) 688-690.

{1.11} B.J. Halperin and D.R. Nelson, Phys. Rev. Lett. 41 (1978) 121; Phys. Rev. Lett. 41 (1978) 519;
D.R. Nelson and B.J. Halperin, Phys. Rev. B19 (1979) 2457;
D.R. Nelson, Phys. Rev. B18 (1978) 2318;
B.J. Halperin and D.R. Nelson, Proceedings of the Second USA-USSR Light Scattering Symposium, New York, May 21-25, 1979 (Plenum Press, to be published).

{1.12} A.P. Young, Phys. Rev. B19 (1979) 1855.

{1.13} V.L. Berezinksii, Sov. Phys.-JETP 34 (1971) 610;
F. Wegner, Z. Phys. 206 (1967) 465.

{1.14} J.M. Kosterlitz, J. Phys. C7 (1974) 1046.

{1.15} J. Oitmaa and D.D. Betts, Can. J. Phys. 56 (1978) 897.

{1.16} C.J. Coombs and J. Oitmaa, Finite Cell Calculations for the Anisotropic Heisenberg Antiferromagnet, to be published.

{1.17} L. Marland and D.D. Betts, Ground State Properties of the s=½ XY Ferromagnet on the Triangular Lattice, submitted to Physics Letters.

{1.18} M. Suzuki and S. Miyashita, Can. J. Phys. 56 (1978) 902.

{1.19} D.D. Betts and D. Cutheil, in Theoretical Chemistry: Advances and Perspectives, vol. 6, eds. H. Eyring and D. Henderson (Academic Press, to be published) especially Sec. VII.

{2.1} Daniel C. Mattis, Phys. Rev. Lett. 42 (1979) 1503.

{2.2} W. Marshall, Proc. Roy. Soc. A232 (1955) 48;
E. Lieb, T. Schultz and D. Mattis, Ann. of Phys. (N.Y.) 16 (1961) 407;
E. Lieb and D. Mattis, J. Math. Phys. 3 (1962) 749.

{2.3} L. Jansen and M. Boon, Theory of Finite Groups-Applications in Physics (J. Wiley and Sons, New York, 1967) 40 and 239.

{2.4} A. Ralston, A First Course in Numerical Analysis (McGraw-Hill, New York, 1965).

{2.5} J. Oitmaa and D.D. Betts, Can. J. Phys. 56 (1978) 897;
see also M. Suzuki and S. Miyashita, Can. J. Phys. 56 (1978) 902.

{2.6} L. Marland, personal communication.

{4.1} M. Suzuki, Prog. Theor. Phys. 56 (1976) 1454;
see also E. Fradkin and L. Susskind, Phys. Rev. D17 (1978) 2637.

{4.2} D.D. Betts, personal communication.

{4.3} D.R. Nelson and J. M. Kosterlitz, Phys. Rev. Lett. 39 (1977) 1201.

{4.4} J.V. Jose, L.P. Kadanoff, S. Kirkpatrick and D.R. Nelson, Phys. Rev. B16 (1977) 1217.

{4.5} Physics Today, Aug. 1979, pps. 18-20.

{4.6} J. Rudnick, Phys. Rev. Lett. 40 (1978) 1454.

{4.7} D.J. Bishop and J.D. Reppy, Phys. Rev. Lett. 40 (1978) 1727.

{4.8} D.J. Halperin and D.R. Nelson, Proceedings of the Second USA-USSR Light Scattering Symposium, New York, May 21-25, 1979 (Plenum Press, to be published).

{4.9} C.C. Grimes and G. Adams, Phys. Rev. Lett. 42 (1979) 795;
D.S. Fisher, B.J. Halperin and P.M. Platzman, Phys. Rev. Lett. 42 (1979) 798.

{4.10} R.L. Carlin, letter to D.D. Betts.

{4.11} L.J. de Jongh and A.R. Miedema, Adv. Phys. 23 (1974) 1;
H.A. Algra, L.J. de Jongh, W.J. Huiskamp and R.L. Carlin, Physica 83B (1976) 71;
D.D. Betts, Physica 86-88B (1977) 556.

APPENDIX I

TWO SPIN CORRELATIONS IN THE GROUND STATE OF THE XY MODEL ON THE SQUARE LATTICE FINITE CELL RESULTS

In Chapter II only those two spin correlations which were needed for the calculation of the vorticity and pair vorticity operators were presented. A large number of such correlations have been calculated however and Table AI.1 is a compilation of both transverse and longitudinal correlations for finite cells on the square lattice. The correlations for even N cells were calculated by Dr. J. Oitmaa , as part of the research described in {1.15} while those for odd N cells were calculated as part of the research described in this thesis. The correlations are defined as

$$C_T(r/\delta) = \langle S_o^x S_r^x \rangle = \frac{1}{4}\langle S_o^+ S_r^- + S_r^+ S_o^- \rangle \quad , \tag{AI.1}$$

and $$C_L(r/\delta) = \langle S_o^z S_r^z \rangle \quad , \tag{AI.2}$$

where $\vec{S}$ is a spin ½ operator and δ is the lattice spacing. The values of r/δ listed in the table are those for which these correlations are independent. For example, for N=10, each site has two distinct first and second-nearest neighbours, while there are no independent third-nearest neighbour pairs and only 16 fourth-nearest neighbour pairs. For N=8, there are only first, second and third-nearest neighbours, 16 pairs of each. Five figures are included and an uncertainty of $\pm\ 1.0\times10^{-5}$ due to machine errors may be assumed.

Table AI.1 - Transverse and longitudinal correlations in the ground state of the spin ½ XY model on finite cells of the square lattice.

N	r/δ	$C_L(r/\delta)$	$C_T(r/\delta)$
4	1	-0.12500	0.17678
	$\sqrt{2}$	0	0.12500
5	1	-0.05000	0.15000
8	1	-0.05398	0.14657
	$\sqrt{2}$	-0.01136	0.13078
	2	-0.01136	0.13078
9	1	-0.04652	0.14371
	$\sqrt{2}$	-0.00904	0.12493
10	1	-0.05029	0.14402
	$\sqrt{2}$	-0.00958	0.12686
	$\sqrt{5}$(16)	-0.01050	0.12192
13	1	-0.04440	0.14070
	$\sqrt{2}$	-0.00707	0.12393
	2	-0.00622	0.12105
16	1	-0.04558	0.19062
	$\sqrt{2}$	-0.00663	0.12171
	2	-0.00663	0.12171
	$\sqrt{5}$	-0.00585	0.11696
	$\sqrt{8}$	-0.00444	0.11445

Table AI.1 - Transverse and longitudinal correlation in the ground state of the spin ½ XY model on finite cells of the square lattice. (Continued)

N	r/δ	$C_L(r/\delta)$	$C_T(r/\delta)$
18	1	-0.04445	0.13988
	$\sqrt{2}$	-0.00629	0.12196
	2	-0.00513	0.11819
	$\sqrt{5}$	-0.00542	0.11744
	3	-0.00486	0.11590

APPENDIX II

GXYSQDATA and GXY4COR

In this brief appendix the content of the files GXYSQDATA and GXY4COR, which have been placed in the Statistical Physics Program and Data Library, will be discussed. Only a description of the contents of these files is presented. Details can be obtained from the files themselves, which have been documented for this purpose.

The file GXYSQDATA contains all the data which has been generated by finite cell calculations on the square lattice. For N=8,9,10 and 13 this includes the elements of the space group S_N, the basis states and their symmetry numbers, the matrix elements of $-H_{XY}/J$ in this basis and the eigenvalues and eigenvectors of this matrix. Because of the large size of the Hamiltonian matrix for N=16 and 18, only the greatest eigenvalue and the corresponding eigenvector are recorded for these cells. In addition the limitations of storage space prevented the Hamiltonian matrix elements for the N=18 cell from being written into a permanent file. These therefore are not present in GXYSQDATA. A list of nearest neighbour pairs, for each N, is also present in this file. Together with a knowledge of the cell geometry, this data allows the numbering of each cell which was used to be reproduced. This knowledge is important for the interpretation of the elements of S_N and the basis states in geometric terms. The line format of each piece of data is recorded in the file.

The program file GXY4COR contains the program written to evaluate four spin correlations of the form

$$\langle \phi_o^{(N)} | (il,jk) + (ik,jl) - (ij,kl) | \phi_o^{(N)} \rangle \quad , \qquad \text{(AII.1)}$$

where

$$(ij,kl) = S_i^+ S_j^+ S_k^- S_l^- + S_k^+ S_l^+ S_i^- S_j^- \quad . \qquad \text{(AII.2)}$$

The dimension and format statements included are appropriate for calculations on 16-spin cell data. As input, the program requires the elements of S_N, the basis states and their symmetry numbers and the coefficients of the ground state eigenvector in this basis. This data, for all N, is present in GXYSQDATA. For any $N \leq 13$, the program is designed to calculate up to five correlations of the form (AII.1). The numbers i,j,k and l are specified directly in the program and need not be included in the input file. For N=16 limitations of central core space which is available to an individual program prevents more than two such correlations from being evaluated, during one run of the program. For N=18 and 19 (the latter being the dimension of a cell on the triangular lattice) only one correlation of the form (AII.1) can be computed during one run. An interesting feature of the program is that, just as it allows the direct calculation of (AII.1) which involves a sum (and difference) of correlations of the form

$$\langle \phi_o^{(N)} | (ij,kl) | \phi_o^{(N)} \rangle \quad ,$$

any ground state correlation of the type

$$\langle \Phi_o^{(N)} | a_1(ij,kl) + a_2(i'j',k'l') + a_3(i''j'',k''l'') + \ldots | \Phi_o^{(N)} \rangle ,$$

where a_1, a_2, a_3 are any numbers and the sets $\{i,j,k,l\}$, $\{i',k',k',l'\}$ and $\{i'',j'',k'',l''\}$,... are all distinct, can be calculated with small modification to GXY4COR. In the case of, e.g. N=19, this feature will allow the direct calculation of the sum of the two four spin correlations involved in <p'> in approximately the same amount of time as the computation of one such correlation would require. Because of the large amounts of time involved in these calculations such a saving may outweigh any advantage in calculating both correlations involved separately.

APPENDIX III

ON THE GROUND STATE OF THE ANTIFERROMAGNETIC PLANE ROTATOR MODEL

By analogy with the ferromagnetic plane rotator model introduced in Chapter I, the antiferromagnetic plane rotator is defined by the Hamiltonian

$$H = J \sum_{<i,j>} \vec{S}_i \cdot \vec{S}_j = J \sum_{<i,j>} \cos(\phi_i - \phi_j) \quad , \qquad \text{(AIII.1)}$$

where the coupling constant J is positive and ϕ_i is the angle made by the spin vector $\vec{S}_i$ with some reference axis. The vector $\vec{S}_i$ is assumed to have unit magnitude. The minimum energy configuration of spins which interact according to this Hamiltonian is such that neighbouring spins $\vec{S}_i$ and $\vec{S}_j$ are anti-parallel, or as close to anti-parallel as possible. Now both the square and hexagonal lattices can be divided into two sub-lattices, A and B, such that all the nearest neighbours of a particular spin on one sub-lattice belong to the other sub-lattice. The antiferromagnetic ground state is then clearly that state in which all the spins on sub-lattice A are oriented in one direction and all the spins on sub-lattice B are oriented in the opposite direction. Each nearest neighbour interaction $\vec{S}_i \cdot \vec{S}_j$ is then -1 and the resulting energies per site, -2J on the square lattice and -3/2J on the hexagonal lattice, are minimal. Note that there is a degeneracy in this type of state, in the sense that the angle of the spins on sub-lattice A with respect to a fixed reference axis can assume any value in the range 0 to 2π rad.

This degeneracy is of course shared with the ferromagnetic version of (AIII.1).

The same procedure cannot be applied to the triangular lattice which can in fact be divided into a minimum of three geometrically similar sub-lattices. This lattice however may be regarded as constructed out of unit triangular cells and the construction of the ground state begins with the determination of the minimum energy configuration of one such cell. With the cell vertices numbered 1, 2 and 3, and taking the spin on site 1 to define a reference axis, the cell Hamiltonian can be written as

$$H_{cell} = J(\cos\theta_2 + \cos\theta_3 + \cos(\theta_2-\theta_3)) \quad , \qquad \text{(AIII.2)}$$

where the angles θ_2 and θ_3 are measured with respect to the reference axis. Minimizing this expression as a function of θ_2 and θ_3 leads to the following two distinct solutions for θ_2 and θ_3:

$$\theta_2^{(1)} = -2\pi/3 \quad , \; \theta_3^{(1)} = +2\pi/3 \quad , \qquad \text{(AIII.3)}$$

and

$$\theta_2^{(2)} = +2\pi/3 \quad , \; \theta_3^{(2)} = -2\pi/3 \quad . \qquad \text{(AIII.4)}$$

With a positive angle corresponding to counter-clockwise rotation, and with a numbering of vertices as in Figure 3.4, it is easy to see that the solution $\theta_2^{(1)}$, $\theta_3^{(1)}$ represents the vortex configuration of Figure 3.4(a)1. While the solution $\theta_2^{(2)}$, $\theta_3^{(2)}$ corresponds to the antivortex configuration of Figure 3.4(b)1. Again there is a degeneracy implicit in the two configurations represented by these solutions, in

the sense that the orientation of the spin on site 1 is arbitrary. Given that the spin one one site of a unit triangular cell has an arbitrary, fixed direction, two configurations that have the same, minimum, energy can be constructed. One is a vortex and the other is an antivortex. These are generated by first numbering the vertices of the cell so that the positive direction coincides with 1 2 3 (as in Figure 3.4), where site 1 is the location of the fixed spin. A vortex is constructed on this cell by placing the spin on site 2 at an angle of $-2\pi/3$ rad. with respect to the fixed spin on site 1, and the spin on site 3 at the same angle of $-2\pi/3$ rad. but now with respect to the spin on site 2. The original spin on site 1 is "automatically" oriented at an angle of $-2\pi/3$ rad. with respect to the spin on site 3. An antivortex is constructed by following the same procedure with a displacement angle of $+2\pi/3$ radians.

It is now possible to construct the ground state of the antiferromagnetic plane rotator on the triangular lattice and understand why it is the minimum energy state. First divide this lattice into three sub-lattices, A, B and C as shown in Figure AIII.1. Place all the spins on sub-lattice A parallel to each other and oriented in some arbitrary direction. Then place all the spins on sub-lattice B in a direction rotated by $-2\pi/3$ rad. with respect to the orientation of the spins on the A sub-lattice. The spins on the C sub-lattice are then oriented at an angle of $-2\pi/3$ rad. with respect to the spins on the B sub-lattice. Now each triangular cell on the lattice belongs to one of six classes, with

respect to the orientation of the site spins as each cell is traversed in a positive direction; these are ABC, BCA, CAB, ACB, CBA and BAC. The first three and last three are easily seen to correspond to degenerate energy states, since the energy of a unit triangular cell depends only upon the relative orientation of the spins about this cell. The form ABC corresponds to a vortex by construction so the form ACB must correspond to an antivortex, as can be seen from Figures 3.4(a)1 and (b) 1. Now it was shown above that the vortex and antivortex configurations are degenerate in energy and that this energy was the minimum possible for a unit triangular cell. Because each and every such cell on the lattice of Figure AIII.1 is in the minimum energy configuration, this entire lattice is in a minimum energy configuration.

The ground state so derived is illustrated in Figure AIII.2 for a particular choice of the direction of the spins on sub-lattice A. It is interesting to note that this state consists of vortices and antivortices packed into the lattice so that each vortex (antivortex) is adjacent to three antivortices (vortices). No plaquette, in the terminology of Chapter III, has zero vorticity. Another interesting feature of this state, mentioned in Chapter III, is that if it is regarded as constructed out of "upright" triangular cells with vortex configurations of spins, antivortex configurations will appear in the "inverted" triangular cells which appear as the "upright" cells are joined together to form the

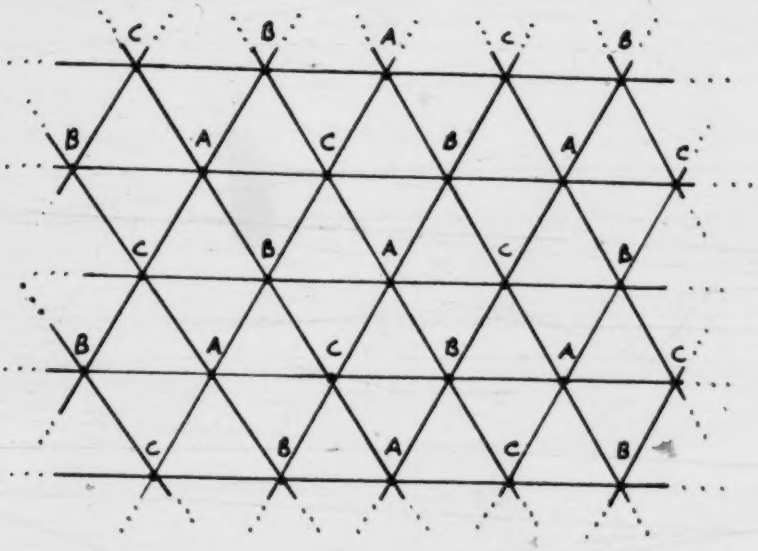

Figure AIII.1 - Triangular lattice partitioned into three geometrically similar sub-lattices.

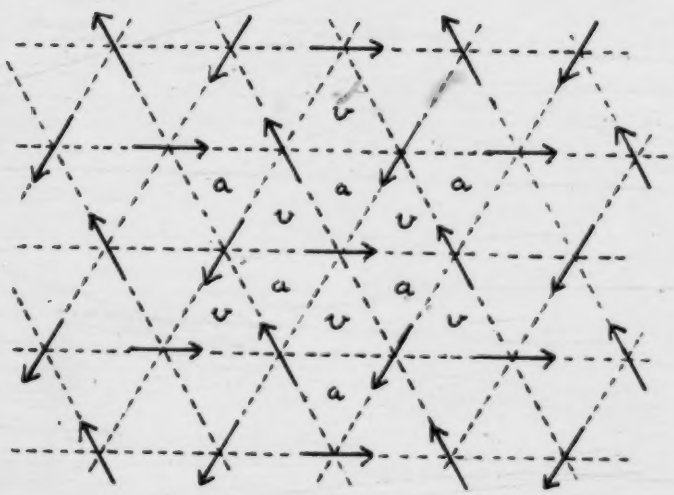

Figure AIII.2 - Antiferromagnetic ground state of the plane rotator model on the triangular lattice (v≡vortex, a≡antivortex).

infinite lattice. It thus appears that the triangular lattice cannot be tiled with vortex configurations alone without generating antivortices as well, although the geometry of the vortex and antivortex cells is slightly different, as noted in Chapter III.